Journal of Sol-Gel Science and Technology (2020) 94:505–530
https://doi.org/10.1007/s10971-020-05222-1

REVIEW PAPER: NANO-STRUCTURED MATERIALS (PARTICLES, FIBERS, COLLOIDS, COMPOSITES, ETC.)

Check for updates

# Customized hydroxyapatites for bone-tissue engineering and drug delivery applications: a review

Gurdyal Singh[1] · Ravinder Pal Singh[2] · Sukhwinder Singh Jolly[1]

Received: 14 November 2019 / Accepted: 7 January 2020 / Published online: 17 January 2020


## Abstract

Hydroxyapatite (HAP, $Ca_{10}(PO_4)_6(OH)_2$) remains to be the foremost choice in biomedical field right from repair/replacement for the damaged hard tissues to be acting as effective drug delivery agent for tissue healing. Though, HAP is similar in composition with the mineral component of bone, some issues such as lack of mechanical and antimicrobial properties, low degradation, lesser drug loading capability, lower stimuli responsiveness, and targeted deficiency have continuously posed major challenges. However, enactment of various physicochemical, biological, mechanical properties can be improved by articulating particles morphology, size, structure, porosity, synthesis technique, and ionic substitution into HAP structure. Unique structure of HAP permits various anionic and cationic substitutions. Among the available synthesis routes, hydrothermal and microwave-assisted techniques seem to be the most suitable techniques to synthesize HAP with close control over desirable properties. This review primarily focuses on highlighting the customization of desirable properties by controlling particles size, morphology, synthesis parameters, and substitution of mono/multi ions into HAP structure to obtain a product appropriate for bone-tissue engineering and drug delivery applications.

## Graphical Abstract

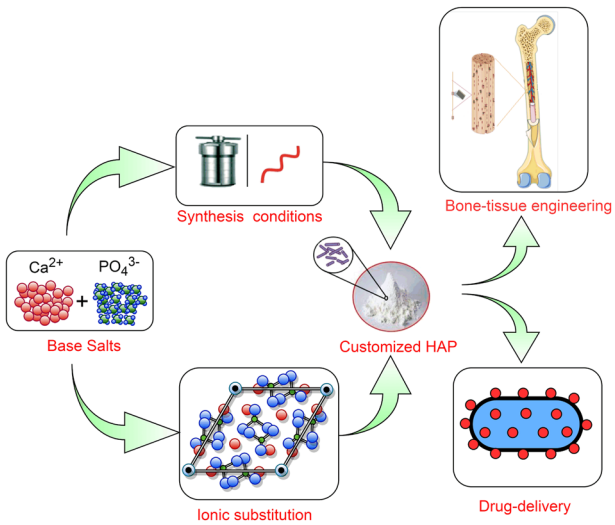


✉ Gurdyal Singh
gurdyalvirk@gmail.com

[1] Department of Mechanical Engineering, Sri Guru Granth Sahib World University, Fatehgarh Sahib, 140407 Punjab, India

[2] School of Mechanical Engineering, Lovely Professional University, Phagwara, 144411 Punjab, India

**Keywords** Hydroxyapatite · Ionic substitution · Microwave · Hydrothermal · Bone-tissue engineering · Drug delivery

**Highlights**

- Effect of particle size and morphology on desirable properties of hydroxyapatite is explored.
- Influence of hydrothermal and microwave synthesis techniques and their governing parameters are discussed in detail.
- Role of mono and multi ionic substitution to control the desirable properties is discussed.
- Use of tailor-made hydroxyapatite is reviewed for bone-tissue engineering and drug delivery applications.

## 1 Introduction

Biomaterials are widely used to treat, evaluate, restore and/or replace any tissue, organ, or function of the body, which in turn improve the quality and span of human life. Biomaterials offer promising solutions and can be used in the human body to substitute or support the damaged parts [1]. Materials closely resemble to biological apatite are easily digested and dissolved in the host tissue without any adverse effects. Therefore, materials with chemical composition and molecular structures similar to natural living tissue(s) offer good replacement. These materials have proven their usage to replace or restore functioning of body tissue and can work continuously or intermittently in contact with body fluids. Biomaterials can be obtained either from nature or can be synthetically prepared in laboratory using variety of chemical methods involving metallic compounds, polymers, ceramics, or composite materials. These synthetic biomaterials had proven their usage ranging from hard tissue engineering to the drug delivery applications [2].

This paper comprehensively discussed the desirable properties of hydroxyapatite as biomaterial and customization of its properties by controlling particle size, morphology, and selected ionic substitution. This review is divided into number of sections. The first section presents introduction and general knowledge about biomaterials, specifically elaborating hydroxyapatite and its desirable properties. The second section focuses on customization of properties by tailoring size, shape, and ionic substitution. The third section discusses the role of most commonly used synthesis technique viz. hydrothermal and microwave and their operating parameters. The applications of customized hydroxyapatite nanoparticles in bone-tissue engineering and drug delivery field are discussed in fourth section. Finally concluding remarks are presented with future scope.

## 2 Types of biomaterials

Biomaterials in general can be categorized into four major groups: biometals, bioceramics, biopolymers, and biocomposites. Application of particular biomaterial is affected by the mutual biological reaction and adaptability between the selected biomaterial and the host body.

### 2.1 Biometals

Biometals and alloys are generally used as load-bearing implants to replace or support the hard tissue. Titanium, stainless steel, and their alloys have been used since long as bone/joint replacements, dental implants, surgical instruments etc. Superior mechanical properties and biological inertness are the important characteristics of biometals, but at the same time it lacks biocompatibility, which raises various associated problems in terms of degradation, disintegration, bonding with soft tissue, harmful metal ions release in body, low bending strength, and metal corrosion etc. [3].

### 2.2 Biopolymers

Polymers are generally made of small repeating units or isomers bonded together to form long chain molecules [4]. These long chain molecules are formed either by primary covalent bonding or by secondary bonding forces such as vander waals along the backbone chain. Polymers are fabricated into linear, network, or branched structures depending on the functionality required from the repeating units. Several types of synthetic polymers are used as biomaterials, including polymethylmethacrylate (PMMA), polyethylene, polystyrene, and polyvinylchloride. Polymers offer wide range of physical and mechanical properties with lower density as compared with metallic and ceramic materials. Bioresorbable or biodegradable polymeric implants eliminate the drawbacks associated with metal or alloy implants, such as foreign body reactions, mechanical properties in excess of the host tissue, and subsequent surgeries to remove metallic implants. However, degradation rate of these biopolymeric materials is not equivalent to the growth rate of new bone [5]. Currently, biopolymers are used for different applications such as artificial organs, medical devices, aids treatment and diagnosis, restorative devices, smart biological systems, etc.

### 2.3 Biocomposites

Composite is usually referred to the materials containing two or more distinct constituent materials or phases. These constituent components govern the physical and mechanical properties of composites and hence, these are more beneficial in comparison with homogeneous materials. In-fact, human hard tissues are in the form of inorganic–organic nanocomposites [6]. In particular, properties of a composite material depend on the size and morphology of the heterogeneities, volume fraction occupied by them, and the interface among the constituents. Among composite materials, ceramics and polymer based composites have exhibited promising application as a biomaterial such as HAP/collagen, HAP/chitosan–gelatin, HAP/chitosan/PMMA etc. [6].

### 2.4 Bioceramics

Bioceramics is a large class of inorganic nonmetallic materials and include range of applications for repairing and replacing hard tissues such as bones, hip-joints, and teeth. The important characteristics of bioceramics include biocompatibility, antimicrobial activity, bonding with soft tissue, no foreign body response from host, and resistance to pH change. These had reported better host tissue response than polymers or metals [7]. Bioceramic materials generally include ceramics, bio-glasses, and glass-ceramics. Over the past few decades, bioceramics such as hydroxyapatite, tricalcium phosphates, alumina, zirconia, and bioactive glasses have undergone significant advancements to improve human life by offering reliable solutions to health care industry [8]. Bioceramics for orthopedic applications have gained significant importance because of associated problems of the other biomaterials such as steel, cobalt alloys, and poly (methyl methacrylate) [3]. To overcome associated problems and to find suitable replacement, significant attention has been drawn to bioceramics. Bioceramics exhibit excellent biocompatibility, chemical stability, non-toxicity, superior corrosion resistance, mechanical strength, and hence have been actively employed in orthopedic applications since past few decades [9]. Depending on their bioactivity, all these biomaterials can be generally categorized into three main groups as mentioned in Table 1.

## 3 Calcium phosphates

Calcium phosphate (CaP) bioceramics are widely preferred as bone graft material in hard tissue engineering. These materials are synthesized in numerous forms ranging from granules, dense to porous particles, and even used as coatings in dental and skeletal prosthetic applications. These are easily accepted by host tissues because of the excellent osteointegration and biocompatible properties. The main reasons for the use of CaP in biomedical applications are attributed to its similarity in phase composition and structural parameters with natural hard tissue, which assist in formation/growth of new bone apatite, non-toxicity, and bioresorbabilty to surrounding tissues.

Several CaP compounds can be derived (Table 2) to suit any particular environment on the basis of the constituents, their valence, and position in the crystal lattice. The stability of CaP compounds is controlled by calcium to phosphorous ratio, processing temperature, amount of water present in the compound, and pH of the surrounding environment. Their structural and spectroscopic properties along with toxicity are the deciding parameters for their applications as suitable biomaterial.

Among the listed CaPs, hydroxyapatite is the most stable, bioactive (osteoconductive), non-toxic, non-immunogenic material and as a result most favored for use in biomedical applications [10].

## 4 Hydroxyapatite

Hydroxyapatite (HAP, $Ca_{10}(PO_4)_6(OH)_2$) is the most important CaP compound found as mineral phase in natural hard tissues. HAP acts as a reinforcement in natural hard tissues and is responsible for the stiffness of bone, enamel, and dentin. In cortical (compact) bone, its crystals are found within collagen as needles oriented in the direction of the fibers. HAP can be derived from synthetic or natural resources. Synthetic HAP with stoichiometric composition

**Table 1** Properties and applications of biomaterials according to their bioactivity

| Biomaterials | Definition | Examples | Applications |
|---|---|---|---|
| Bioinert | Stable, minimal interaction with surrounding tissues | Stainless steel, titanium, and alumina | Joint prostheses, hip prostheses, dental implants |
| Bioactive | Degrade gradually, interactions with surrounding hard and soft tissues | HAP, bioactive glass, and glass ceramics | Bone and dental filling |
| Bioresorbable | Materials slowly dissolve in body and replace damaged tissues/organs | Chitosan, gelatin, and polylacticpolyglycolic acid copolymers | Tissue engineering |

**Table 2** Various CaP compounds with formula and Ca/P ratios [22]

| Name | Formula | Ca/P | Acronym |
|---|---|---|---|
| Amorphous calcium phosphate | n/a | n/a | ACP |
| Tetracalcium phosphate | $Ca_4O(PO_4)_2$ | 2.0 | TetCP |
| Hydroxyapatite | $Ca_{10}(PO_4)_6(OH)_2$ | 1.67 | HAP |
| Tricalcium phosphates (α, β, γ, and δ) | $Ca_3(PO_4)_2$ | 1.50 | TCP |
| Octacalcium phosphate | $Ca_8H_2(PO_4)_6{\cdot}5H_2O$ | 1.33 | OCP |
| Dicalcium phosphate dihydrate | $CaHPO_4{\cdot}2H_2O$ | 1.0 | DCPD |
| Dicalcium phosphate | $CaHPO_4$ | 1.0 | DCPA |
| Calcium pyrophosphate | $Ca_2P_2O_7$ | 1.0 | CPP |
| Calcium pyrophosphate dihydrate | $Ca_2P_2O_7{\cdot}2H_2O$ | 1.0 | CPPD |

of Ca/P = 1.67, has attracted much consideration for hard tissue engineering due to its resemblance with the mineral constituents of mammalian bone and teeth [9]. It is least degradable form of CaP bioceramics with excellent bioactivity and biocompatibility [9, 11]. HAP has demonstrated strong chemical bonding with hard tissues [12] due to osteoconductive, nontoxic, nonimmunogenic nature [7], thus offers greater benefits in biomedical applications compared with other bone substitute materials.

## 4.1 Structure of HAP

Crystallographic structure of HAP can be categorized as monoclinic or hexagonal as per the space group. Monoclinic structure of HAP is not stable and can be destabilized even by the presence of a small quantity of ions [13], so it is of less practical importance as compared with hexagonal structure. Whereas, hexagonal form of HAP is stable and found in most biological apatites, but in nonstoichiometric composition [14]. The unit cell parameters of crystal structure are $a = b = 9.418$ Å and $c = 6.884$ Å [15]. Due to the presence of $OH^-$ group, it is called hydroxyl-apatite or sometimes referred as calcium phosphate hydroxide. The unit cell of HAP forms a sixfold symmetry with $c$-axis perpendicular to other three equivalent axes ($a_1$, $a_2$, and $a_3$) at angles 120° to each other as shown in Fig. 1. The $Ca^{2+}$, $PO_4^{3-}$, and $OH^-$ groups make up the closely packed hexagonal unit cell giving a molecular formula $Ca_{10}(PO_4)_6(OH)_2$ [16]. The structure is formed by $PO_4$ tetrahedral arrays retained by Ca ions intermingled among them. Ca occupies two different sites, Ca (I) and Ca (II) in hexagonal structure. Out of ten Ca atoms in HAP structure, four atoms are positioned at Ca (I) and other six atoms at Ca (II) site. The configuration can be pronounced as a phosphate assembly parallel to the $c$-axis, intersected by $OH^-$ ion filled parallel channels. Ca (I) site atoms have different

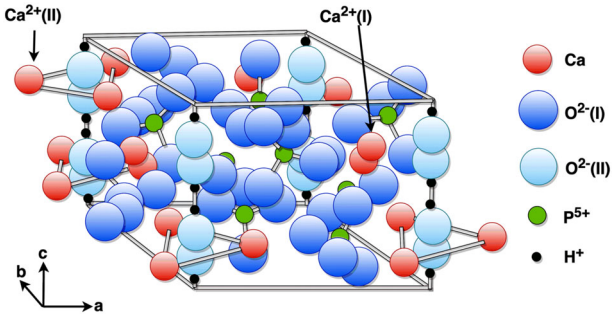


**Fig. 1** Crystallographic structure of unit cell of HAP [206]

environments and are positioned in columns parallel to $OH^-$ channels. Ca (II) atoms organized in staggered triangular arrays, formed the channel walls. Ionic substitution can readily occur in these channels, which may account for the high degree of substitution to mimic natural apatite [13, 17]. The unit cells of HAP are structured along $c$-axis, thus offering oriented growth preferred to obtain needle or rod shape morphology [18].

## 4.2 Properties of HAP

Unique properties of synthetic HAP have justified its use as biomaterial for hard tissue repair and replacement. The degree of crystallinity, size, morphology, chemical composition, synthesis technique, and their aggregates, plays crucial role in influencing HAP properties, in situ response, and potential applications.

### 4.2.1 Biological properties

HAP has been widely used as artificial bone substitute because of its favorable biological properties including: biocompatibility, nontoxicity, bioaffinity, bioactivity, osteoconduction, osteointegration as well as osteoinduction.

**4.2.1.1 Biocompatibility** Biocompatibility is the ability of a material to perform its desired function with respect to a medical therapy, without causing any adverse local or systematic effects in the recipient, but at the same time, producing the most suitable beneficial tissue response in that specific situation and thus optimizing the clinically relevant performance of that therapy [19]. Cytotoxicity is the quality of being toxic to cells. HAP is considered to be noncytotoxic and biocompatible due to its similarity in chemical composition with the bone. The biocompatibility of HAP surfaces can be evaluated using cell–-material interaction studies such as attachment, proliferation, and differentiation. Yoshimura et al. [20] synthesized nontoxic and biocompatible fibers or whiskers of HAP using hydrothermal method. Zhao et al. [21] synthesized rods-like and spherical shape HAP particles and determined the effect

of HAP nanoparticles and their morphology on osteoblasts growth by the MTT method. Results demonstrated higher absorbency value on the surface with spherical morphology.

**4.2.1.2 Bioactivity** It is the ability of the material to directly bond with bone surface through formation of carbonate apatite as a result of ion-exchange reactions, dissolution, and precipitation with the physiological environment. Biodegradability is the ability of a material to be decomposed or broken down by a biological organism. Bioresorbability is the ability of a material to be gradually dissolved or resorbed by cellular and/or metabolic process. The apatite layer formation mimics the type of interface formed when natural tissues repair themselves, thus enables an implant to bond directly to host-tissue without requirement of physical or mechanical attachment. HAP possessed excellent bioactive characteristics, which is further function of chemical stoichiometry, surface morphology, and crystallinity [22].

**4.2.1.3 Osteoconduction** It means that bone grows on a surface. It is generally used in conjunction with implants to act as scaffold or template to guide the newly forming bone on its surface or down into pores, pipes, or channels [23]. Osteoconductive materials permit bone cell attachment, proliferation, migration, and phenotypic expression, leading to formation of new bone-tissues, thus creating a strong interface.

**4.2.1.4 Osteointegration** It is the stable anchorage of an implant achieved by the formation of bone-tissue surrounding the implant without the growth of fibrous tissue at the bone–implant interface [23].

**4.2.1.5 Osteoinduction** It means the recruitment of immature cells and the stimulation of these cells to develop into mature osteoblasts. This process is generally a part of fracture healing and is accountable for the majority of newly formed bone-tissue after bone fracture or an implant incorporation [23]. HAP surface characteristics support osteoblasts cell adhesion, differentiation, and bone growth by creeping substitution from adjacent living bone. Extensive research has been done over the past several years to better understand the biological potential of HAP [24].

### 4.2.2 Mechanical properties

Despite its excellent biocompatibility, HAP material has been limited mostly to non-load-bearing applications because of its modest mechanical properties. HAP is subjected to rapid wear, failure, and premature fracture of implants [25]. To become viable bone replacement material, mechanical properties of HAP need to improve to the level of natural bone as listed in Table 3 but without compromising its biocompatibility.

**Table 3** Properties of both HAP and natural bone [9]

| Mechanical properties | Natural bone | HAP |
|---|---|---|
| Young's modulus (GPa) | 7–30 | 40–120 |
| Compressive strength (MPa) | 10–230 | 300 |
| Bending strength (MPa) | 200 | 110–200 |
| Fracture toughness ($MPa/m^{1/2}$) | 2–12 | <1 |
| Poisson's ratio | 0.30 | 0.27 |

Various methodologies have been extensively investigated to enhance the mechanical properties of HAP, which include adding dopants [26, 27], making composites [28, 29], and controlling microstructures [30]. Mechanical properties reported to be improved by synthesizing HAP particles on nanodimensional scale, since the nano-sized HAP particles exhibit apparently superior mechanical properties in comparison with the micron-sized counterparts [31].

### 4.2.3 Antibacterial properties

Antibacterial property is very important characteristic desired to reduce the chances of implant failures by providing resistance against infection, thus ensuring long term stability. Lack of antibacterial properties is also one of distinct limitations of pure HAP. Major research is directed toward improving the antibacterial property of HAP by substitution of suitable ions into HAP structure [32]. As it has been proved that certain metal ions can penetrate into the bacterial cells and deactivate their enzymes whereas some other metal ions can kill bacteria by generating hydrogen peroxide [33]. The other way to improve the antibacterial properties of pure HAP is to modify its structure for optimum loading and release of antibiotic drugs [34].

### 4.2.4 Physicochemical properties

Physicochemical properties are evaluated through physical, structural, and chemical analyses to determine phase purity, size, shape, major element components such as Ca, P, Ca/P molar ratio and presence of other trace elements silicon, magnesium, sodium, potassium, strontium, zinc etc. HAP is a bioactive material that undergoes in vivo ionization and its dissolution rate depends on number of factors including crystallinity, morphological parameters, and processing conditions. HAP is easily soluble in an acidic medium while remains insoluble in an alkaline state. It is slightly soluble in distilled water. Moreover, HAP solubility in any medium changes with the presence of proteins, enzymes, amino acids, and other organic compounds. The biocompatibility between implants and host tissues is influenced by HAP solubility and associated chemical changes, which critically

depends on crystallite size, shape, and porosity. HAP is relatively insoluble under physiological conditions; thus it behaves in thermodynamically stable condition at body temperature [35].

Synthetic HAP has proved itself as proven and reliable alternative for hard tissue engineering, but it has some weakness including variable biological behavior at macroscale, low-load-bearing strength, low degradation rate etc. Though, pure HAP possessed good osteoconductivity and biocompatibility, still it lacks adequate bioactivity, osteoinductivity to induce osteoblasts, osteogenic differentiation of the stem cells to stimulate new tissue formation, which is vital for restoration of bone defects and tissue engineering [36]. These shortcomings can be improved and superior HAP with customized properties can be formulated by controlling the parameters discussed in next sections.

## 5 Customization of HAP properties

Despite chemical similarity of synthetic HAP with natural apatite, potential replacement is limited due to inherent limitations including lack of osteoinductivity, low degradation rate, poor mechanical and antibacterial properties etc. In addition, biological response in the form of bone regeneration, cell adhesion and spreading, proliferation, and differentiation etc. are functions of HAP material characteristics, such as crystallinity, morphology, porosity, and suitable ionic substitutions [37]. Therefore, to obtain peculiar physicochemical, structural, and biological properties; precise control and customization are of critical importance for potential applications.

### 5.1 Effect of particle size on HAP properties

One of the approaches to improve the performance of synthetic HAP is by exploring the unique advantage offered by nanotechnology. In this regard, uniquely structured HAP particles with size <100 nm in at least one dimension is perceived to be helpful and potentially ideal for orthopedic applications. Nanodimesional HAP is the main mineral component of natural bone. HAP in bone is in the form of nanodimensional sized, needle shaped crystals having ~5–20 nm width and 60 nm length, embedded in collagen fiber matrix with poorly crystallized nonstoichiometric apatite phase [38]. Due to physical and chemical similarities with the natural apatite, nano-form possesses exceptional biocompatibility and bioactivity to bone cells and tissues. The structures of natural bone apatite can be accurately mimicked and replaced by formulating oriented aggregation of nanodimensional HAP particles.

As compared with the bulk materials, physical and chemical properties of nanomaterials are totally governed by their particle size and shape. Thus, synthesizing HAP particles to nanodimensional size offered superior functional properties of the replaced tissue, due to large surface-area to volume-ratio and quantum effects generated due to discrete nano structure. This improves the contact reaction and the stability at the artificial/natural bone interface. Therefore, nanodimensional domain is very important area to study. From the biomimetic point of view, significant improvements in biological properties have been observed when crystallite size of HAP approaches to nanoscale. Smaller crystals of nanodimensional phase offered better proliferation and viability of various cells. Thus, synthesizing HAP particles to nanodimensional scale offers great potential to revolutionize the biomedical field starting from hard tissue engineering to drug delivery carriers for targeted healing.

Nanodimensional HAP particles have emerged as viable solution to treat the infections by acting as nanocarriers for antibiotics [39], genes [40], proteins [41], and various drugs due to their exceptional bioactivity, biocompatibility, and nontoxicity [42, 43]. Reports suggested that nanodimensional HAP exhibited better interaction at implant–cell interface as compared with microndimensional particles [44]. Compared with the macro size formulations, nanophase HAP particles exhibit properties, such as grain size, pore size, surface area, wettability etc., which influence protein interactions in the form of bioactivity, adsorption, configuration, thus regulating subsequent osteoblasts adhesion and long-term functionality [45]. More to the point, nanodimensional HAP has shown better bioactivity than coarser crystals [46]. Use of nanodimensional HAP reported to promote the bone remodeling process by enhancing osteoclasts (bone-resorbing cells) functions at implant surface [45]. Furthermore, it has been demonstrated that nano-HAP particles with diameters of ~20 nm have shown best effect on promotion of cell growth and inhibition of cell apoptosis on human osteoblast-like MG-63 cells in vitro as compared with ~80 nm [47].

Despite variety of applications for dental and orthopedic repair and restoration, conventional HAP exhibits poor mechanical properties, which limits its use. It is believed that nanodimensional HAP, when densified with nanoscale grains, provide improved strength. It has been well documented that mechanical properties of nanopowders are governed by its particle size, orientation, and morphology [30]. Nanodimensional HAP particles have exhibited improved mechanical properties as compared with microndimensional counterparts [48]. Significant improvements in bending properties, such as bending modulus, bending strength, flexural rigidity, and bending structural stiffness have been exhibited by nanodimensional HAP particles due to changes in surface porosity, grain boundaries, crack initiation sites, which makes it preferable orthopedic and

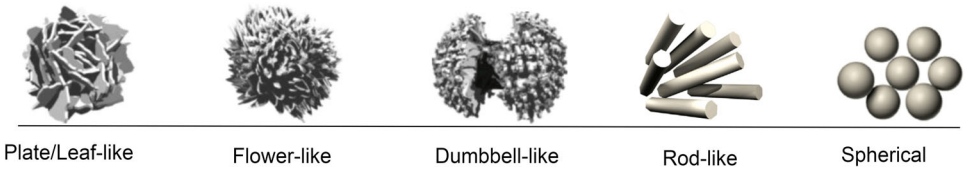


**Fig. 2** Different forms of particle morphology

dental implant material [49]. Mechanical properties, such as hardness and toughness of nanodimensional HAP particles appeared to increase with the reduction of grain size from micrometer to nanometer scale [31]. HAP nanoparticles (~67 nm) exhibited higher surface roughness (17 nm) as compared with surface roughness of 10 nm shown by micron-dimensional particles (~180 nm). High surface roughness enhances osteoblast functions by influencing the bonding strength. Interfacial interaction between HAP nanoparticles and various substrates has shown that bonding strength is not only effected by the nature of functional groups on the substrate but also by surface roughness matching between nanoparticles and substrate [50]. Studies revealed that nanodimensional HAP has significantly lower contact angles (6.1) in comparison with the submicron-dimensional HAP (11.51) particles.

In addition, nanodimensional HAP particles provide porous structure with the diameter of individual pores reported to be very small (~ 6.6 Å) than that in the microndimensional HAP particles (19.8–31.0 Å) [51]. Porous structure improves the osteoinduction as compared with the particles having smooth surfaces and nonporous structure [52]. Particles of nanocrystalline structure offer large surface area, which in turn improve the sinterability and increased densification [53]. The specific surface area of nanodimensional HAP particles exceeds 100 $m^2/g$, whereas their counterpart micro-dimensional particles have lower surface area (typically 2–5 $m^2/g$), thus offering poor sinterability [54]. Nano-structured hierarchical designs of HAP have shown higher drug loading and favorably release characteristics [55]. Nanoparticle based drug delivery systems have proven their ability to deliver larger quantity of drug (high payload), prolonged drug life, improved drug solubility and have shown sustained, stimuli-responsive, targeted drug releasing abilities [56]. In situ incorporation of ciprofloxacin into HAP nanoparticles exhibited antibacterial ability of HAP against *S. aureus* and *E. coli* bacteria causing osteomyelitis without compromising bioactivity and cytocompatibility of HAP particles [34].

Contemporary research has been directed toward the development of nanodimensional HAP formulations accurately mimicking the natural hard tissue for better biocompatibility, but at the same time improving the other lacking properties, such as strengths etc., aiming for better and more effective biomaterial.

### 5.2 Effect of particle morphology on HAP properties

Morphology is the form of study comprising size, shape, and structure. Functionality of nanoparticles can be effectively controlled by controlling their morphology. Morphology like plate-like, flower-like, rods-like, spheres-like as shown in Fig. 2, can be obtained by controlling synthesis technique and its controlling parameters. HAP particles with different morphologies have exhibited different performances.

In recent years, nanorods-like morphology of HAP particles has gained a lot of consideration. Natural bone is a nanocrystalline, inorganic material with rods-like microstructure [57]. Several studies confirmed that one-dimensional structure substantially enhance the mechanical properties of nanopowders by offering dense microstructure with high strength and fracture toughness (such as nanorods, nanowires, and nanofibers) [58]. Nanorods-like particle morphology not only possessed desirable bioactivity and biocompatibility but also better absorbability, as underlying Van der Waals interactions are proportional to the large area offered by the rods [11].

It has been reported in recent studies that diverse nanostructures have different loading and releasing efficiencies for specific drugs [59]. Therefore, amount of drug absorbed and release mechanisms can be regulated by developing particular nanostructure of HAP particles. Researchers have reported that narrow particle morphology (nanorods) to be more advantageous over spherical counterparts in targeted drug delivery applications, as they adhere more effectively to endothelial cells [60]. Rods-like crystals exhibit large surface area as compared surface area of hexagonal crystals faces, which positively affect the adsorption property, thus proved to be effective drug carriers with enhanced protein adsorption due to greater charging surface efficiency [61]. Nanorods-like structure has demonstrated better drug loading and controlled release properties for ibuprofen drug [62]. The micron and mesoporous carbonated HAP microspheres have also exhibited good drug loading efficiency [59]. Studies revealed that physical structure of HAP particles influenced the production of the pro-inflammatory cytokine IL-18 in human monocytes. Needle-shaped particles have demonstrated the greatest influence on production of IL-18 and other inflammatory cytokines as compared with spherical and other irregular shaped particles [63]. High aspect ratio of

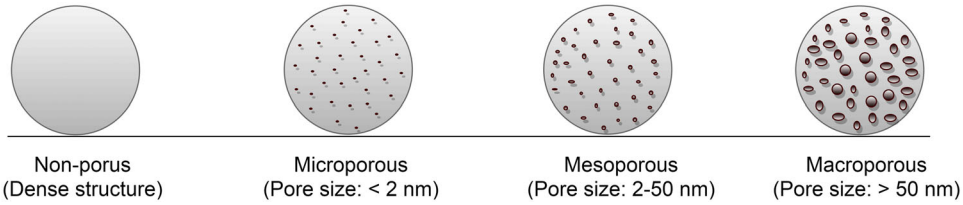


**Fig. 3** Classification of porous structures [207]

nanorods-like morphology has shown increased specific attachment and reduced nonspecific attachment to their target compared with their spherical counterparts [64].

Nanoparticles with porous structure offer large specific surface area, large pore volume, number of internal and external surfaces that offer good bonding with host tissues as well as very good carriers for drugs and proteins, thus showing wider application prospects [65]. Porous structures can be categorized into macroporous, mesoporous, and microporous depending upon pore-size as shown in Fig. 3. Studies of porous CaP nanospheres observed that larger and agglomerated porous spheres could delay drug release process, thus can be used as perfect drug carrier for the therapy of skeletal disease [66]. Porosity of HAP structures has proved to be a crucial factor, not only for efficient and targeted drug delivery but also vital for other histological responses associated with bone and bone-tissue ingrowth. Although porous structures have shown much higher drug loading and release characteristics, but at the same time, strength of structure decreased with the increase in porosity [67]. Compressive strength has been influenced not only by the total porosity, but also by the pore size [68]. So, there must be proper balance between strength and porosity of HAP structures to achieve required mechanical properties with optimum drug loading capacity.

## 5.3 Effect of ionic substitutions on HAP properties

Pure HAP is considered to be incompetent for use in bone-tissue engineering applications, especially in load-bearing applications, due to inherent brittleness and lack of strength. Another important limitation is the high degree of crystallinity, which reduce degradability of pure HAP when embedded into the tissues. The composition and structure of HAP depend on the presence of the substituted ions [16]. It has been reported that the biological response of pure HAP can be improved to suit a particular environment by doping/substitution of HAP with suitable ions. Inclusion of specific elemental substitution alters the crystal structure, improves biocompatibility and bioactivity, enhances the osteoclasts and osteoblasts response, which further help in bone regeneration processes [25]. The substitution of physiologically relevant ions into HAP structure positively influences the physicochemical properties such as osteoconductivity, crystallinity, solubility, thermal stability

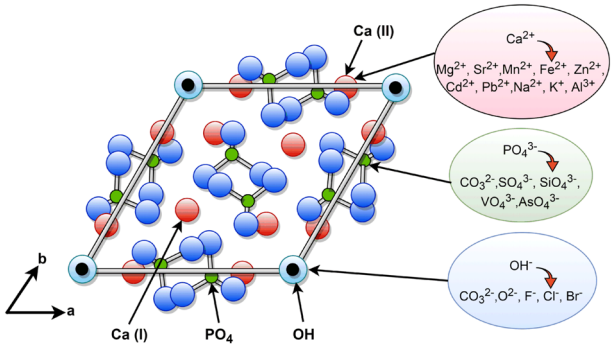


**Fig. 4** Various ions substitution site in HAP structure projected along c-axis [208]

[69, 70], lattice parameters [71], and improve its biocompatibility and bioactivity [72]. Also, research on ions substitutions in HAP is relevant and useful to better understand biomineralization process, critical properties, increase in bioactivity, and acting as drug carrier to treat bone infections. Therefore, studies regarding synthesis of nanodimensional HAP and its substitution with the various ions have become the subject of interest since last few decades.

A variety of cationic and anionic substitutions into HAP structure are possible due to high flexibility and stability offered by HAP structure as shown in Fig. 4. It has been demonstrated that desirable properties of synthetic HAP can be enhanced by the incorporation of selected ions such as cations ($Sr^{2+}$, $Zn^{2+}$, $Na^{+}$, $Mg^{2+}$, $K^{+}$, $Mn^{2+}$) or anions ($F^{-}$, $Cl^{-}$, $HPO_4^{2-}$, $SiO_4^{4-}$ or $CO_3^{2-}$) into its lattice structure [73]. These substitutions play crucial role in the biological activity influencing particle morphology, structural size, solubility, and surface chemistry of HAP [74]. These substitutions induce specific biological responses on cells [70]. HAP crystal structure can accommodate substitutions of $Ca^{2+}$, $PO_4^{3-}$, and $OH^{-}$ groups by various other ions.

### 5.3.1 Cationic substitutions

Cationic substitutions can replace $Ca^{2+}$ ions in HAP crystal structure. Some cations that can be substituted into HAP include $Sr^{2+}$, $Zn^{2+}$, $Mg^{2+}$, $Mn^{2+}$ etc. The cations with radius smaller than $Ca^{2+}$, such as $Zn^{2+}$, $Mg^{2+}$ and $Mn^{2+}$ accommodate in site Ca (I), while larger radius cations like $Sr^{2+}$ accommodate in site Ca (II) [16]. Properties of HAP

including crystal structure, morphology, stability, solubility, surface charge, and bioactivity are affected due to the incorporation of such cations [13]. Hence, effects of substitution of some key cations on HAP properties have been discussed in this section.

*Magnesium (Mg)* is the fourth most abundant cation found in the human body. It is reported to play a significant role in bone metabolism by stimulating osteoblast proliferation, in particular during the initial stages of osteogenesis and its depletion causes bone fragility [75]. It positively affects osteoclasts, osteoblasts activities, and thereby influences bone growth. Substitution of Mg ions inhibits the nucleation and growth of HAP crystals [17, 76]. Its incorporation into HAP lattice causes lattice distortion and reduction in lattice dimensions due to its smaller ionic radii (0.065 nm). Its incorporation for Ca in HAP crystal structure occurs up to 10 mol% occupying Ca (II) positions [77, 78]. Mg-substituted HAP showed decrease in crystallinity with the increase in Mg content [78, 79]. Its incorporation into HAP exhibits increased solubility in comparison with pure HAP [80]. It has been reported that Mg incorporation positively affects the hydration state on HAP surface, resulting into retention of more water molecules at their surface [81]. As far as mechanical properties are concerned, compressive strength and micro-hardness reported significant decrease with the incorporation of Mg content up to 1.8 wt% [82]. On the other hand, fracture toughness increased with Mg substitution up to 0.6 wt%. Furthermore, experimental studies revealed reduced grain size and increased porosity of HAP structure owing to Mg substitution [82, 83].

*Strontium (Sr)* is another cation present as trace element in bone and plays a vital role in mineralization of bone-tissues [84]. Inclusion of $Sr^{2+}$ ions into HAP lattice has shown improved biocompatibility and bioactivity due to increased solubility, thus reported to promote osseointegration process [85]. Recent studies revealed that incorporation of $Sr^{2+}$ into HAP structure enhanced osteoblasts and inhibited osteoclasts activity during bone remodeling process [32, 84]. However, in vitro studies disclosed that bone cell interaction varies with $Sr^{2+}$ concentration level, which simulate osteoblast activity in low range (3–7 wt%) but decreases with the increase in $Sr^{2+}$ level [69]. As compared with pure HAP, mechanical properties have also shown significant improvement with the substitution of $Sr^{2+}$ into HAP [86]. Kim et al. reported increase in vickers hardness with the addition of $Sr^{2+}$ ion. [87]. Antibacterial properties have seen improvement with addition of $Sr^{2+}$ [32]. Furthermore, amount of $Sr^{2+}$ substitution strongly influences the lattice parameters and crystallinity of HAP crystals. Various reports have demonstrated that lattice parameters (both *a*-axis and *c*-axis) have increased steadily with the increase of $Sr^{2+}$ content into HAP crystal structure. However, little/no effects have been observed on crystalline phases of HAP at low $Sr^{2+}$ ion concentration (<1.5 wt%) [27]. $Sr^{2+}$ addition has resulted into nanorods-like morphology, which resemble with natural bone mineralogy and proved to be effective medium for targeted drug delivery [88]. Porous nanodimensional material with better resorption has been reported with the addition of $Sr^{2+}$ ions [72]. Thus, evidence of effectiveness of $Sr^{2+}$ substitution on structure and properties of HAP has aroused interest of researchers toward Sr substitution in HAP.

*Zinc (Zn)* is known to be an important mineral of natural apatite. Zn is reported to enhance bone formation by osteoblast proliferation, biomineralization processes [89, 90]. It is involved in numerous enzyme reactions, including DNA and RNA replications and protein synthesis. Zn assists in various metabolic mechanisms responsible for normal bone growth and development and its deficiency results in decrease in bone density [91]. However, biological performance of Zn is dependent on its release behavior. The ions release required during bone-tissue regeneration should be controlled and slow [92]. As ionic radius of Zn (0.075 nm) is smaller than Ca (0.099 nm), it can be quantitatively substituted into HAP lattice at Ca(II) site by direct synthesis exposed to mild conditions [93]. Its doping into HAP lattice improves thermal stability, regulates morphology and crystallinity [94]. Inclusion of Zn inhibits the growth of HAP crystals and stoichiometry is no longer maintained because Ca/P ratio decreases on increasing Zn mol%. Crystal strain reported to increase with the increase in Zn concentrations, which further reduces the crystallite size [94] and decreases crystallinity with increasing Zn content [95]. Zn-substituted HAP exhibits irregular morphology, with agglomerates grow in size with increasing Zn amount. The Zn-substituted HAP powders showed high phase purity up to 800 °C, beyond which β-TCP started to appear [73]. FTIR analysis showed that $HPO_4^{3-}$ increased whereas $OH^-$ decreased with the increase in Zn amount [73]. In vitro analysis in simulated body fluid showed the formation of CaP layer at the periphery of the Zn-substituted HAP particles. This biologically active layer improves the chemical bonding between HAP and bone [96].

*Cerium (Ce)* exhibits behavior similar to Ca in organisms. It has been reported to accumulate in small amounts in bones and assists in stimulation of metabolism in organisms. Previous researches have indicated that Ce possesses antibacterial properties and can play a vital role in preventing caries [97]. Doping of $Ce^{2+}$ ions into HAP structure increased solubility, which further helped to improve antibacterial properties and biodegradability. Decrease in crystallinity and crystal size have been reported upon substitution of $Ce^{3+}$ ions. Furthermore, particle morphology changed from nanorods to long needles with increasing Ce

content [98]. Ce doped HAP coatings has demonstrated good biocompatibility and encouraged osteoblast cell affinity [99]. However, only limited studies have been reported so far on Ce-doped HAP particles to ascertain its effect on HAP properties and, thus requires further exploration.

*Manganese (Mn)* is another important cation responsible for various metabolic mechanisms of bone and greatly influences the bone remodeling process. Its deficiency in bone causes various deformities, such as decrease in bone length and thickness [100]. Mn ions replace Ca ions up to one atom per unit cell in HAP structure (5.5 wt%) at Ca (I) position, causing slight rotation of $PO_4^{3-}$ ions [101]. Substitution of Mn in HAP showed inhibitory effect on crystallization [100, 102]. In Mn-substituted HAP, partial transformation of HAP into β-TCP occurred at 600 °C as Mn entered β-TCP phase more easily than HAP phase. Calcination of Mn substituted HAP showed decrease in lattice parameters of β-TCP as compared with HAP [103]. In vitro tests of Mn-substituted HAP have shown no cytotoxicity effect with osteoblasts cells [104]. In addition, Mn-substituted carbonated HAP coatings deposited on titanium substrates reported to assist in metabolism activation, osteoblast differentiation, and proliferation [105].

### 5.3.2 Anionic substitution

Generally, most appropriate anionic substitutions in HAP involves substitution of $CO_3^{2-}$ for $PO_4^{3-}$ or $OH^-$ groups and $F^-$ for $OH^-$ groups [106]. The trivalent anionic phosphate sites cannot accept vacancies, because the trivalent anions are quite large and vacancies destabilize the lattice [107]. An important feature of HAP is the occurrence of hydroxyl ions in same unit cell. The anions such as $F^-$, $Cl^-$, $HPO_4^{2-}$, $SiO_4^{4-}$ or $CO_3^{2-}$ are used for substituting hydroxyl and phosphate groups, respectively in the HAP lattice. Anionic substitutions like $PO_4^{3-}$ groups by $HPO_4^{2-}$ and $CO_3^{2-}$ and $OH^-$ by $F^-$ reported to improve the surface properties and modify the thermal stability of HAP [108].

*Carbonate ($CO_3^{2-}$)* Biomimetic HAP contains significant amount of $CO_3^{2-}$ ions. Presence of $CO_3^{2-}$ ions in HAP increases its solubility as well as resorption rate relative to pure HAP [109]. Incorporation of $CO_3^{2-}$ replaces $PO_4^{2-}$ ions, thus increases the Ca/P molar ratio beyond 1.67, which results into nonstoichiometric HAP, known to be less thermally stable [110]. Substitution of $CO_3^{2-}$ inhibits HAP crystal growth resulting into poorly crystalline structure with enhanced solubility [17].

*Fluorine ($F^-$)* exists in human bones and teeth as an essential element against dissolution. The presence of fluorine in blood plasma and saliva is essential for normal skeletal and dental development. It is homogeneously distributed in bone-tissue and within the thin outer layer of tooth enamel. Substitution of $F^-$ ions into HAP structure stimulates the formation of bone-tissue and thus improves osteoblast response in terms of adhesion, differentiation, and proliferation processes compared with pure HAP. Its substitution assists bonding between bone and implant and strengthens bone structure [111]. As it offers low solubility, thus helps to prevent demineralization of bone. It also provides good acid resistance that is necessary for teeth [112]. Appropriate amount of $F^-$ promotes mineralization and crystallization of HAP in bone forming process, whereas high $F^-$ concentration in bone can lead to severe adverse effects like osteomalacia [113]. $F^-$-substituted HAP exhibits good biocompatibility, low solubility, and better thermal and chemical stability than pure HAP [114]. Moreover, $F^-$ substitution can cause an increase in crystallinity, decrease in crystallite size and crystal strains of HAP [115].

*Silicate* is one of the essential trace element present in bone and has been reported to play key role in biomineralization process, osteoblast differentiation, osteoclast development, and resorption activities, thus accelerating metabolism between bone and host tissues. The simplest route for Si inclusion in HAP is the substitution of $SiO_4^{4-}$ ions for $PO_4^{3-}$ groups. Previous researches have suggested that substitution of Si improved the biocompatibility of HAP for bone regeneration by offering osteointegration. Bioactivity of HAP improved after incorporation of Si [116]. The addition of Si in HAP crystal structure inhibited the crystal growth and confirm the reduction in crystallite size [117, 118]. Bioreactivity has also shown improvement as compared with pure HAP after Si inclusion in crystal structure [119]. Besides, substitution of Si has shown to supply the essential ions helpful in biological interaction for bone regeneration [120, 121]. Si-substituted HAP undergoes faster dissolution preferentially around the grain boundaries and promotes biomimetic precipitation of HAP by creating crystalline defects by charge compensation [122]. Si substitution helps to create finer HAP microstructure by influencing electronegativity on surface [123]. Moreover, mechanical properties like diametral tensile strength improved for Si-HAP particles [124]. However, high Si level (<2 mol%) has shown reduction in crystal size, which resulted into fast dissolution of the implants, thus not suitable for bone cell attachment for prolonged time periods [125]. The amount of Si incorporation into HAP is beneficial to maximum value of 5 wt% [116, 126]. It has been reported that about 1 wt% is enough to induce key bioactive improvements. Si-HAP coatings have shown their potential in terms of drug delivery vehicles [127]. High reactivity of Si-substituted HAP has been attributed with the increase in thermal ellipsoid dimension of H atoms present parallel to the *c*-axis [18].

*Sulfate* is another essential anion employed for reconstruction of skin cells, nails, hairs, and cartilage. It is

reported to be fourth most abundant anion in blood plasma and is important for proper functioning of human cells [128]. Alshemary et al. [129] successfully substituted sulfate ions into HAP structure via microwave irradiation technique by varying concentrations of $SO_4^{2-}$ in the range of $x = 0.05$–0.5, using Ca $(NO_3)_2{\cdot}4H_2O$, $(NH_4)_2HPO_4$, and $Na_2SO_4$ as starting materials. Results confirmed the nano-dimensional (41 nm) needle shaped morphology with homogenous and uniform distribution but with reduced crystallinity. Toyama et al. [130] synthesized sulfate-substituted HAP from ACP i.e., $Ca_3(PO_4)_2{\cdot}nH_2O$ and $Na_2SO_4$ using hydrothermal processing at 220 °C for 3 h. They concluded substitution of $HPO_4^{2-}$ ions with $SO_4^{2-}$ ions, due to similarity in radii and valences.

#### 5.3.3 Co-substitution of ions

In order to accurately mimicking of chemical composition and other desirable properties pertinent to natural apatite, synthetic materials must be synthesized with co-substitution or multi-ionic substitutions. These co-substitutions of elements into HAP structure reported to introduce desirable effects of more than one ion/element on various properties as compared with pure or mono-ionic-substituted HAP particles. In co-substitution, simultaneous substitution of both cationic and anionic elements has been reported. It involves the substitution of cations like $Sr^{2+}$, $Ce^{2+}$, $Na^+$, $Zn^{2+}$, $Mg^{2+}$, $Mn^{2+}$, etc. for $Ca^{2+}$ sites accompanied by the substitution of $PO_4^{3-}$ by $CO_3^{2-}$, $SiO_4^{4-}$, or $OH^-$ by $F^-$. This co-substitution ensures the neutrality of apatitic structure. The cation–anion co-substitution in HAP reported to affect its morphology, lattice parameters, crystallinity, and crystallite size. Essential trace elements like Mg, Na, F, K, Cl, and $CO_3^{2-}$ etc. of natural bone have been successfully co-substituted to produce the materials with favorable properties [131]. Results have demonstrated enhanced degradability and improved drug loading and release characteristics as compared with pure or single ion doped HAP materials. When two or more elements are doped in HAP structure, the substituent can have a synergistic or antagonistic effect on the properties of HAP. For example, $Mg^{2+}$ and $CO_3^{2-}$ co-substitution exhibited synergistic effect on the crystallinity and dissolution properties of synthetic HAP, whereas, $CO_3^{2-}$ and $F^-$ have antagonistic effect with $F^-$ being more dominant.

*Strontium and magnesium* co-substitution destabilized the HAP structure. Increase in Mg content showed increase in β-TCP phase, both with and without Sr co-substitution [132].

*Magnesium and Zinc* co-substitution in HAP crystal structure exhibited excellent biocompatibility and biological properties [93]. Co-substitution of these ions destabilized the apatitic structure, increased HAP crystallization, and reduced the decomposition temperature of HAP. Incorporation of $Zn^{2+}$/$Mg^{2+}$ ions partially substituted the $Ca^{2+}$ ions in apatite lattice, thus decreased the crystallite size and crystallinity of HAP particles. The substitution limit is reported between 15 and 20% for Zn and <10% for Mg.

*Magnesium and Fluorine* co-substituted HAP ($Ca_9Mg(PO_4)_6(OH)_{2-y}F_y$), ($y = 0$, 0.5, 1, 1.5, and 2) has shown that structural and sinterability properties depend on $F^-$ concentration and calcination temperature [133]. For temperature between 950 and 1250 °C, calcination of samples without $F^-$ and low concentration of $F^-$ ($y = 0.5$) occurred due to solid state diffusion mechanism, while in the samples with higher $F^-$ ($y > 0.5$) at 1100 °C, a liquid phase was present, which increased with the increase in calcination temperature. The liquid phase induced crystallization of needle shaped crystals, which reduced the densification of HAP. The substitution of $Mg^{2+}$ ions resulted in reduction of lattice parameters and exhibited better biocompatibility, biological properties than pure HAP nanopowder.

*Strontium and Cerium* co-substitution has shown improvement in bioactivity and antibacterial property [134]. Report on strontium and silicate co-substitution via the hydrothermal technique showed an increase in lattice constants and improved degradability of materials with increased level of substituent [135].

*Sulfate and Strontium* co-substitution has not been reported so far to the best of authors' knowledge, which makes it potential area of research to combine the desirable effects of strontium and sulfate into HAP structure. When doped individually, Sr increased bioactivity and bone remodeling [32, 84], whereas, sulfate improved the cell functionality [128].

## 6 Synthesis techniques for HAP

From the perspective of numerous applications, HAP nanoparticles need to be synthesized by simple and environmental friendly techniques that yield it in large quantities in order to justify their production and use. Nanodimensional HAP particles have been synthesized by a variety of techniques, such as wet chemical [136], sol–gel [137], hydrothermal [138], mechano-chemical [139], solid-state reaction [103], microwave [140], co-precipitation [141], and emulsion techniques etc.

With the use of these techniques, variety of HAP structures, such as particle shape (needles, fibrous, rods, plates, flowers spheres) and size (nanometer, micrometer) can be synthesized [142]. Although various techniques have been reported to synthesize diverse nanostructures of HAP particles, each technique has its own advantages and disadvantages. In case of a sol–gel technique, HAP nanoparticles with high purity and homogeneity can be

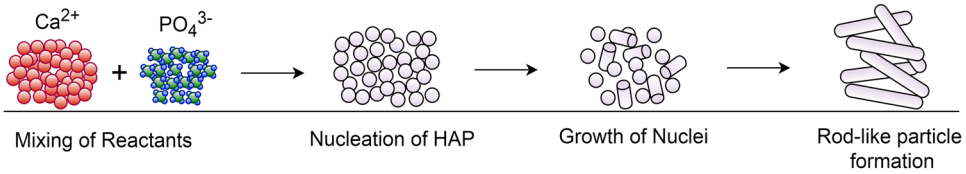


**Fig. 5** Crystallization of rods-like HAP nanoparticles using hydrothermal method [153]

easily obtained using simple devices at low temperatures [143], however, it requires vigorous stirring, long time for hydrolysis, and good pH control. Co-precipitation technique is another simple and low cost technique useful for the synthesis of biomimetic needles-like/nanorods-like or spherical nanoparticles [144]. But, it is associated with low crystallinity, difficulty in process control, and often requires surfactants or polymers to overcome aggregation of particles. Emulsion technique can be used to produce nanoparticles with needles, rods, plates, sphere like morphologies, but, process is complex, time consuming, and requires high sintering temperatures [145]. Mechanochemical technique is another simple and low cost method to produce fibrous aggregates and spherical nanocrystals without high sintering [146], but this technique requires special devices and also produced nanocrystals tend to aggregate. Ultrasonic technique facilitates the fast crystallization and capable of producing nanoparticles having needles-like and spherical morphologies producing low yield and special devices for synthesis [147].

Among these, hydrothermal technique and microwave assisted synthesis techniques have been significantly employed to synthesize nanocrystalline HAP powders owing to their reported advantages over the other techniques. Hydrothermal technique has shown its potential to produce highly pure and homogenous materials [148]. On the other hand, microwave assistant technique is fast and environment-friendly, which leads to the formation of ultrafine nanocrystalline materials [149, 150]. Due to reported benefits, these two techniques have been specifically discussed in detail in the following sections.

## 6.1 Hydrothermal technique

The hydrothermal technique has emerged as one of the most sought-after technique for fabrication of advanced materials, predominantly in the synthesis of highly crystalline, mono-dispersed and homogeneous nanoparticles. Originally, hydrothermal word comes from combination of greek words ‘hydros’ means water and ‘thermos’ means heat energy. Hydrothermal synthesis is described as any homogeneous or heterogeneous reaction taking place in the presence of solvents (aqueous or non-aqueous) under elevated temperature and pressure conditions in a sealed environment to dissolve and recrystallize materials that are relatively insoluble under ordinary conditions [151]. It is used to synthesize supersaturated solutions under high pressure and temperature conditions [152].

Hydrothermal processing of materials generally includes the use of a solvent (usually water with precursor salts), put in a sealed vessel called autoclave, subjected to heating at elevated temperature above boiling point and under pressure that exceeds ambient pressure. By having control over concentration of reactants, nature of solvent, solution pH, hydrothermal temperature, and aging duration, nanoparticles with varied sizes, shapes, and crystallinity can be obtained.

The development of rods-like morphology by utilizing hydrothermal crystallization process generally involves two main stages as represented in Fig. 5. It involves nucleation stage, in which little crystalline cores are framed in a supersaturated medium followed by the growth of nuclei, in which cores ceaselessly develop into the final shape and size of particles [153].

Hydrothermal technique is capable of producing highly crystalline HAP particles in single step without requiring any post treatment in comparison with other methods. Simplicity of operation, higher yield, cost effectiveness, low energy requirement, short reaction times, relatively low-cost reagents, better nucleation control, higher dissolving power etc. are some benefits associated with hydrothermal processing [154]. Furthermore, variety of particle shapes viz. needles, plates, rods-like, spherical with an extensive size distribution can be synthesized by this method [152, 155–159].

The use of surfactants, templates, capping agents, or other organic/biomolecules with hydrothermal processing contribute prominently to the surface adaption of nanoparticles to attain the desired structural and physicochemical characteristics [160]. The reported limitations of hydrothermal technique are its poor control on the precise shape and size of obtained particles, which requires further investigation by controlling the governing hydrothermal parameters. Hence, to examine and optimize these parameters, detailed discussions have been presented in this article.

### 6.1.1 Parameters of hydrothermal synthesis

The particle size, morphology, porosity, and crystallinity of HAP nanopowders obtained using hydrothermal technique are affected by a series of synthesis parameters, such as

nature of precursors and solvents, reaction time, temperature, pH etc., which are explained below:

**6.1.1.1 Nature of precursors** Numerous studies have employed an array of combinations of calcium and phosphorous precursors for hydrothermal synthesis of HAP particles. The synthesis reaction of HAP under elevated temperature and pressure depends largely on the chemical nature of employed precursors. The range of precursors for calcium includes: calcium nitrate tetrahydrate (CNT) [39, 117, 118, 131, 138, 161, 162], calcium chloride [163, 164] etc. The phosphorus precursors include: diammonium hydrogen phosphate [134, 161], ammonium dihydrogen phosphate [39], phosphoric acid [162, 163], sodium monophosphate dihydrate [164], potassium dihydrogen phosphate [138]. The range of precursors for strontium includes: strontium nitrate hydrate [27], strontium nitrate [165, 166], and strontium nitrate hexahydrate [134]. Commonly used precursors for silicon are: $Si(OCH_2CH_3)_4$ (TEOS) [117, 118]. Mostly used precursors for cerium are: cerium nitrate hexahydrate [134] and cerium nitrate [97, 98].

**6.1.1.2 Reaction temperature** Hydrothermal reaction temperature is another critical factor affecting crystallite structure and size control of HAP particles. Zhu et al. [162] reported the effects of different hydrothermal temperatures on morphology of nanoparticles. Results revealed that diameter and length of nanorods increased with the increase in reaction temperature from 140 to 220 °C, whereas, at lower temperature lump shaped particles with small crystal size formed due to lower crystallinity. Thus, it suggested that appropriate rise in temperature is favorable for directional growth of HAP crystal resulting into nanoparticles with high aspect ratio. Liu et al. [152] reported formation of monetite phase at low hydrothermal temperature between 60 and 140 °C for 24 h. Further, nanoparticles with uniform particle size and needles-like morphology having range of aspect ratio between 8 and 20 were obtained at 120 °C. Sadat-Shojai et al. [161] evaluated hydrothermal parameters and reported reaction temperature as most influencing parameter to gain control over physicochemical and structural properties of HAP nanoparticles. According to this study, mean diameter decreased, whereas length, aspect ratio, and crystallinity of nanoparticles increased with the increase in temperature.

**6.1.1.3 Reaction time** Hydrothermal reaction time also plays significant role in controlling the size and crystallinity of HAP particles. Hydrothermal reaction time had no adverse effect on particle size and shape, when subjected to duration between 24 and 72 h. But, longer reaction duration produced monetite as a secondary phase [167]. Zhu et al. [162] investigated the effects of short hydrothermal reaction times i.e., 1, 4, 8, 12 h and reported formation of rods-like HAP particles with the increase in length of nanorods (from 93 to 120 nm) with reaction time. It was reported that supersaturation associated with reaction time was responsible for nucleation and growth of HAP crystals, thus played vital role in controlling the size of particles.

**6.1.1.4 pH** The pH of reactant solution is another important parameter controlling the morphology of particles ranging from whiskers, wires, sheets, rods, and spheres like. Zhu et al. [162] studied the effects of pH on morphology of HAP particles under hydrothermal conditions at 200 °C for 8 h. Results revealed that with increase in pH from 8 to 12, mean diameter of nanorods-like particles increased from 29 to 40 nm, whereas, mean length decreased from 140 to 94 nm. Liu et al. [152] reported whiskers-like particles obtained using hydrothermal treatment of HAP solution at various pH values of 6, 9, and 14. Crystalline HAP whiskers obtained at pH = 6 and 9, whereas, crystallinity decreased at higher pH of 14 at low temperature of 120 °C. Further study demonstrated that mean diameter, length, aspect ratio of nanoparticles decreased, whereas, crystallinity increased with increasing pH value [161].

### 6.1.2 Advantages of hydrothermal technique

End products with unique characteristics such as high purity, crystal symmetry, porous structure, better morphological control, homogenous particle size distributions, wide range of precursors, and solvent compositions, sub-micron to nanoparticles size, dense sintered powders etc. can be synthesized using hydrothermal treatment [151]. Further, this technique facilitates as single-step process, lesser energy requirements, controlled/sealed environment, environmentally benign, avoidance of pollution, low reaction time, lower temperature operations, higher reaction rates, use of larger capacity equipments. In today's world of nanotechnology, hydrothermal technique is clearly on the forefront as compared with other materials processing techniques.

## 6.2 Microwave-assisted technique

Microwave-assisted synthesis is another important technique for rapid and efficient production of nanoparticles. In recent studies, ultrafine, nanostructured, well crystalline HAP particles with high purity have been prepared using microwave-assisted technique [140, 168, 169].

This technique utilizes electromagnetic radiations as the heating source. Interactions between microwaves and dipoles of reactant, force them to align themselves by reorienting to the rapidly changing high frequency electric field, resulting into dielectric heating as schematically

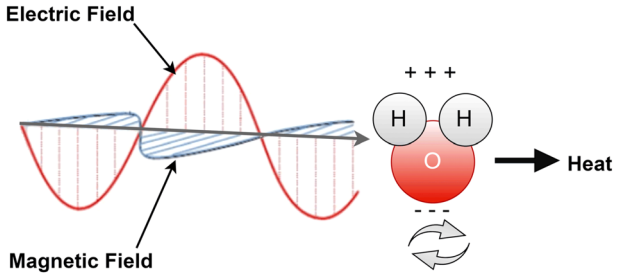


**Fig. 6** Microwave interaction with a dielectric molecule (water molecule) [149]

represented in Fig. 6. Applied frequency is critical parameter for microwave heating to provide suitable response time to dipoles. Frequency of microwaves is important for proper heating. At low frequencies, dipoles get enough time to reorient themselves with the electromagnetic field resulting into small dielectric heating, whereas, at high frequencies, molecular dipoles do not have adequate time to react to high frequency resulting into no movement. Since, there is no motion/rotation of the molecules, which results into no transfer of energy, and hence heating effect does not take place. Therefore, applied microwave frequency is the key point, which plays an important role in the microwave heating and must be suitably chosen as per the response time of dipoles. Mostly, 2.45 GHz frequency has been attributed as optimum microwave frequency reported in literature.

Microwave processing of HAP can be controlled by either refluxing or hydrothermal treatment or under atmospheric conditions (Fig. 7). Kumar et al. [170] synthesized HAP nanostrips of 50–70 nm in diameter and 50–100 nm in length by utilizing microwave refluxing conditions. Liu et al. [171] reported rapid formation of HAP nanostructures by microwave refluxing at 700 W for 30 min. They reported formation of different particle morphologies including nanorods to flower-like nanostructures under different pH conditions. Iqbal et al. [172] synthesized silver-doped HAP nanoparticles under microwave refluxing conditions. Wang et al. [173] prepared HAP nanocrystals by microwave-hydrothermal method in the temperature range of 100–140 °C and reported change in particle morphology from rods-like to prism-like with change in microwave temperature. Siddharthan et al. [174] employed simple microwave under atmospheric conditions to synthesize nanodimensional HAP particles. Alshemary et al. [129] synthesized sulfate-doped HAP needle-shaped nanoparticles with 41 nm size under simple microwave conditions of 800 W for 20 min.

### 6.2.1 Parameters affecting microwave synthesis

In general, it has been observed that size and morphology of HAP particles are governed by pH of reactant solution, microwave power, temperature, and irradiation time.

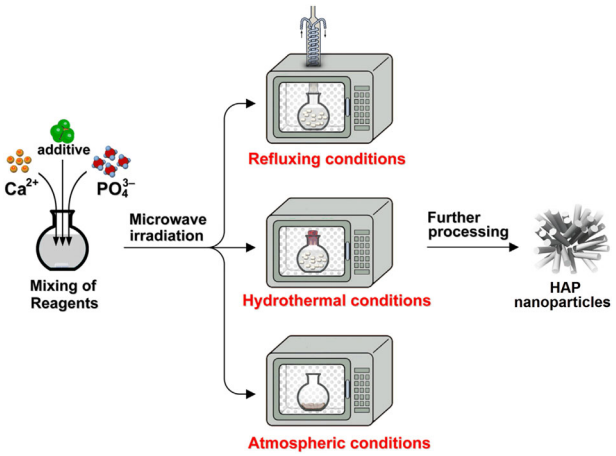


**Fig. 7** Main routes for preparation of HAP nanoparticles via microwave synthesis. Reprinted from Ref. [153] with permission from Elsevier

**6.2.1.1 pH** The pH of reactant solutions holds the key for precipitation of HAP particles. Desired morphology and size of HAP particles can be obtained by regulating the pH media. Nanorods-like particles can be synthesized via isotropic crystal growth at basic pH with elevated temperatures. On the other hand, particles with small size/aspect ratio can be obtained at higher pH with lower temperatures. The HAP precipitation in a slightly basic medium (pH = 7.4), produced particles, which were calcium deficient, irregular in shape, and hundred nanometers in size [175]. Liu et al. [171] rapidly formed HAP nanostructures at different pH values ranging from 9 to 13 under microwave irradiation of 700 W for 30 min. They reported uniform nanorods-like morphology at pH = 9, which changed to flowers-like nanostructures at pH equal to 13. Vani et al. [176] prepared mesoporous nanorods-like particles with 40–75 nm long, 25 nm wide by microwave irradiation at solution pH = 10. Qi et al. [177] synthesized hierarchically structured porous microspheres (0.8–1.5 μm) utilizing microwave-hydrothermal method at 120 °C for 10 min with solution maintained at pH = 10. Zhao et al. [178] reported nanorods assembled hierarchical hollow microspheres at pH = 4.5 by exposing to microwave heating at 180 °C for 5 min.

**6.2.1.2 Microwave power and temperature** The size and shape of HAP nanoparticles can be controlled by choosing suitable microwave power, as dispersion of salt materials in solution increases with the increase in power and hence temperature. Siddharthan et al. [174] investigated the role of microwave power on size and shape of HAP particles by varying microwave power from 175 to 660 W. Results suggested change in morphology of HAP particles from needle shape at 175 W to platelet shape at 660 W, whereas, size of particles showed mixed response with changes in

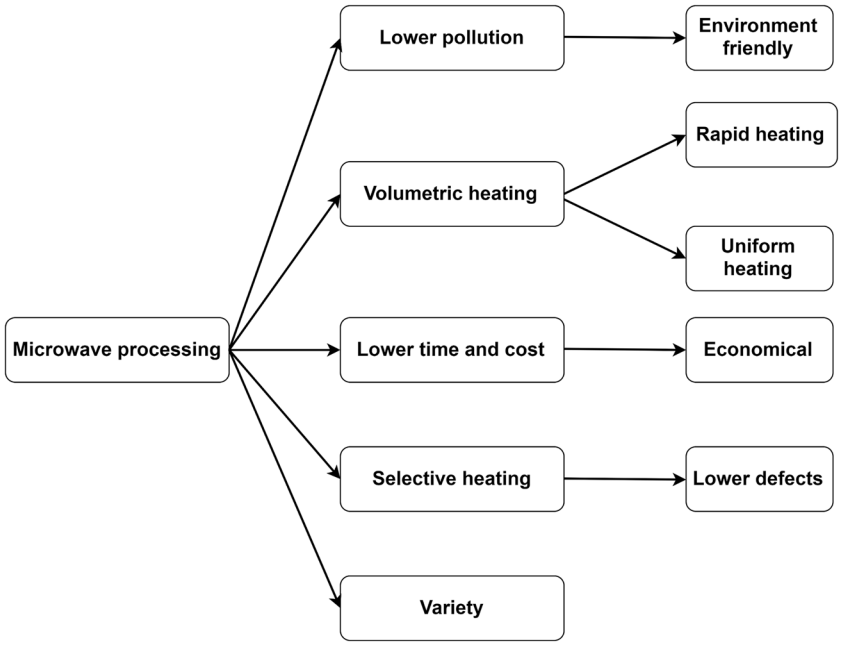


**Fig. 8** Characteristics of microwave processing

microwave power. Singh et al. [179] examined the influence of microwave power (300, 600, 900, and 1200 W) on physicochemical and structural characteristics of HAP particles and reported pure HAP phase with decrease in crystal size, crystallinity, and microstrain with increase in microwave power. Yang et al. [180] investigated the effects of microwave power (70, 210, and 700 W) on thermal stability of HAP and reported stable HAP phase formation at 700 W, whereas, other phases co-exist at lower microwave power heating.

Generally, increasing the reaction temperature greatly reduces the reaction time for HAP formation. Akram et al. [181] reported increase in crystallinity and particle size with the increase in microwave power from 450 to 800 W. Wang et al. [182] investigated the effects of reaction temperature (80, 120, and 140 °C) for 30 min irradiation time using microwave-hydrothermal method and reported formation of hollow microspheres with compact morphology at 140 °C. Qi et al. [177] synthesized hierarchically structured porous microspheres at 120 °C for 10 min using microwave-hydrothermal method. Wang et al. [173] prepared HAP nanocrystals utilizing microwave-hydrothermal method in the temperature zone of 100–140 °C and reported that morphology of HAP particles transformed from rods-like to prism-like structure with the increase of reaction temperature. In most cases, synthesis temperature was not stated due to the unavailability of provision of temperature measurement in domestic microwave ovens.

**6.2.1.3 Irradiation time** Microwave irradiation time has shown significant effects on HAP synthesis. Irradiation time exposure may be continuous [168, 179, 183] or in intervals (on/off cycle) [140, 170, 171, 184, 185]. Continuous irradiation time caused the formation of large size HAP particles as compared with interval heating [184], as continuous microwave heating improved the sintering which stimulated the particle growth or/and their agglomeration [183]. Requirement of irradiation time reduces with the increase in microwave power. Siddharthan et al. [174] reported that irradiation time reduced to 15 min at higher powers (greater than 385 W) as compared with 75 min (175 W). Zhao et al. [178] investigated effects of irradiation time on the morphology of HAP particles. Nanorods-assembled microspheres (<1 μm) with poor crystallinity obtained within 1 min by microwave heating at 180 °C, whereas, when duration of heating time was extended to 30 min, disordered nanorods with average thickness of about 60 nm formed. Thus, it suggested that longer irradiation time led to the development of bigger particles with large aspect ratio. Singh et al. [179] reported decrease in crystal size, crystallinity, and microstrain of HAP particles with the increase in irradiation time.

### 6.2.2 Advantages of microwave synthesis

Microwave synthesis has been reported to be a simple, fast, and effective technique to develop nanoparticles from inorganic materials. Various key characteristics are graphically represented in Fig. 8. As compared with other conventional techniques, microwave has demonstrated its advantages in terms of rapid/homogenous heating, small particle size, accelerating chemical reaction, narrow particle-size distribution, and enhanced crystallinity [174].

Furthermore, it is an energy-efficient, economical, and eco-friendly way to develop ultrafine HAP particles under the green synthesis route [178]. Microwave produces products in relatively very short time by minimizing the thermal gradients and reduction in particle diffusion time. E.g., to prepare HAP powders using sol–gel technique, ageing of reactant solution normally takes 24–48 h at room temperature [57]. On the other hand, in microwave synthesis route, the solution is kept directly into microwave oven for bombardments of microwaves for few minutes only [60]. Within minutes of microwave exposure, bright white precipitates of HAP can be obtained.

### 6.3 Surfactant assisted HAP synthesis

It has been well established that type of precursors and synthesis conditions (both physical and chemical) critically influence the formation of HAP particles. As pH of reactant solution governs the morphology (nanorods, nano-whiskers, nano-sheets/strips etc.) of resultant nanopowders, similarly, presence of chelating agent helps in crystal growth and mediate in HAP nucleation owing to the affinity between the surfactant and HAP crystals [140, 168]. Recent investigations established that use of surfactants is desirable but not compulsory for the formation of HAP nanostructures [186]. Various organic modifiers such as cetyltrimethyl ammonium bromide (CTAB), ethylenediaminetetraacetic acid (EDTA), ethylene glycol, trisodium citrate, tween 20, and citric acid have been tested by researchers to regulate the shape and size of HAP nanocrystals. Among these, EDTA and CTAB have been most frequently used to prepare the nanomaterials with desired structures. Typical formation mechanism for HAP nanorods is represented in Fig. 9.

#### 6.3.1 Effects of EDTA surfactant

It has been reported that EDTA surfactant significantly contributes in controlling HAP morphology by preventing the agglomeration of nanoparticles [140]. Different types of morphologies like nanorods [140], prism-like [138], bow-knot-like, flower-like [171], microspheres [148] have been reported by using EDTA as growth controlling agent by using various synthesis methods like microwave irradiation [169], hydrothermal method [138] etc. Wang et al. [187] prepared nanomaterials with controlled morphology by using EDTA as capping agent by utilizing chemical precipitation method.

#### 6.3.2 Effects of CTAB surfactant

CTAB has been widely used as a nucleation and growth controlling agent to synthesize nanodimensional HAP. Well-crystallized HAP nano-strips were synthesized using microwave irradiation method using CTAB [188]. Mesoporous HAP nanostructure was developed by wet precipitation method at ambient temperature and pressure using CTAB as surfactant [189]. Nanorods with uniform morphology was reported, when CTAB was used under hydrothermal synthesis [160]. Similarly, HAP nanorods were prepared at ambient temperature and pressure conditions by co-precipitation method using CTAB as a chelating agent [141].

## 7 Applications of nanodimensional HAP

Nanodimensional HAP particles have gained significant attention in biomedical field due to their superior structural, physicochemical, biological, and mechanical properties. Researchers have shown great interest because of tremendous applications of these materials in various biomedical areas such as bone-tissue engineering [37], bone fillers [18], soft tissue repairs [190], bioactive coatings [18], protein/gene loading [99], local drug delivery systems [34, 65, 191]. Among these applications, bone-tissue engineering and targeted drug delivery have tremendous potential and therefore, have been discussed in detail in this section.

### 7.1 Bone-tissue engineering

Bone-tissue engineering is a growing field, which deals with therapies for bone remodeling/regeneration. Continuous active research has been carried out to synthesize artificial bone substitute materials that can truly replicate natural apatite for bone repair and regeneration. There has been growing demand for repair or replacement of damaged and diseased parts of human bone, caused due to accidents, sports commitments, problems associated with old age, social life style, and eating habits. High demands of orthopedic surgeries required not only for new patients but

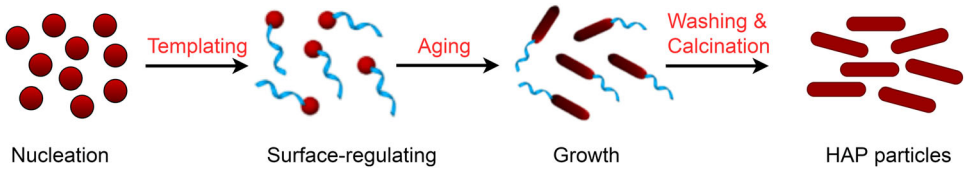


**Fig. 9** Formation mechanism of HAP nanorods assisted by CTAB [153]

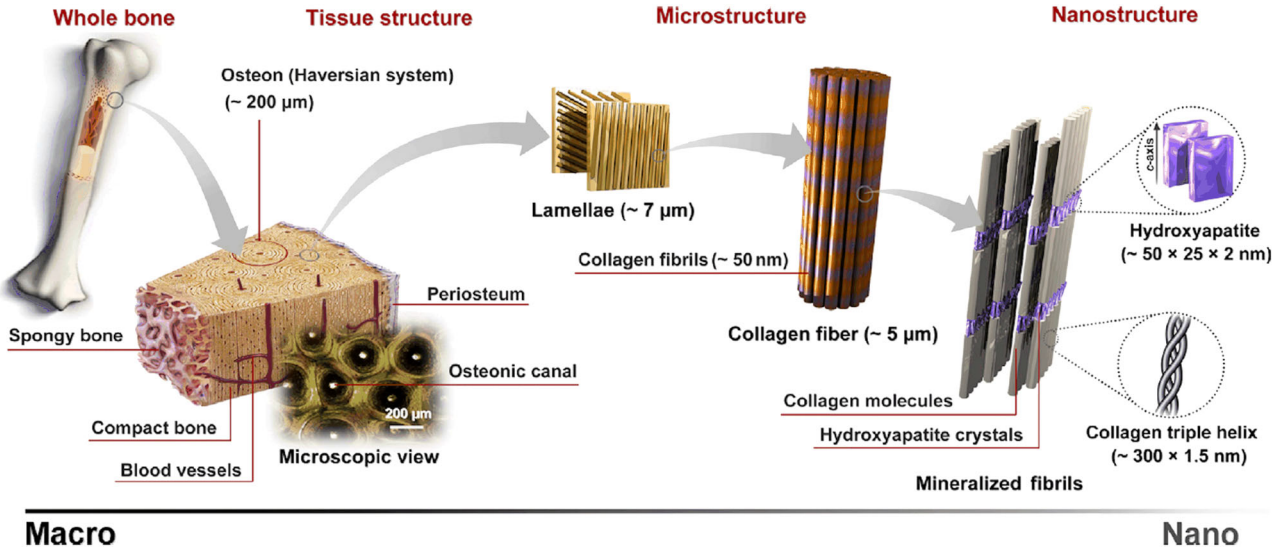


**Fig. 10** Length scales of bones' hierarchical structure. Reprinted from Ref. [153] with permission from Elsevier

also for the ones requiring revised surgeries due to failures caused by instability, infection, wear, osteolysis, in-growth failures, and prosthetic fractures etc.

Natural bone is a composite matrix of organic and inorganic components as represented in Fig. 10. The organic components account for one-third mass of bone that consists of lipids, polysaccharides, and more than 200 proteins [18]. The inorganic component accounts for two-third mass of bone that consists mainly of HAP consisting of 36.6 wt% of Ca and 17.1 wt% of P element with traces of other ions such as $CO_3^{2-}$, $Mg^{2+}$, $Zn^{2+}$, $K^+$, $Na^+$, $F^-$ etc. Precisely, natural bone is calcium-deficient having non-stoichiometric chemical composition (Ca/P molar ratio < 1.67). Bone possesses vacancies, inclusions of foreign anions and cations soaked up from the surrounding body fluids during bone metabolism [192]. Natural bone is nanocrystalline, inorganic materials with rods-like nanostructure [57].

Tissue engineering is an interdisciplinary field that offers suitable biological substitutes to replace, support, maintain, and improve functions of tissues [37]. It involves the use of isolated cells or cell substitutes to replace limited functions of tissue, utilization of tissue-inducing substances, such as growth factors and scaffolds to direct tissue development and other functions of the tissue [37].

Synthetic HAP proposes viable alternative to replace human hard tissues due to chemical resemblance with the inorganic constituent of human bone and therefore has been used for nearly 40 years in orthopedics and dentistry applications for repair and reconstruction [9]. Recent researches showed that synthetic HAP assisted in recovery of damaged bones as well as fostered new tissue formation by bonding with host bone. HAP contributes for strength and resistance under compression, while collagen provides endurance for tensile loading. HAP facilitates greater biological bonding with host tissue as compared with other biomaterials or metallic implants. In vivo studies conducted on rabbits proved that the HAP implants showed new tissue formation and growth by attachment with host bone [37]. Bone grafts fabricated from HAP nanoparticles have been used successfully used for bone-tissue engineering [6]. In addition, biological interactions responsible for bone regeneration such as cell adhesion, differentiation, proliferation etc. are affected by crystallinity, morphology, particle size, and ionic substitutions [37]. Thus advocating the requirement to formulate customized HAP material for tissue engineering applications.

## 7.2 Targeted drug delivery

Materials used for bone-tissue engineering have been gaining significant attention in biomedical applications due to targeted, effective and sustained drug releasing ability [39]. Conventional drug delivery systems reported to have undesirable characteristics such as an instant and rapid drug release, high initial concentration of drug that may reach to toxic level and decreasing dosage over time to a sub-therapeutic level [193]. To achieve the effective concentration of drugs at the targeted area, high dosages are given, which may produce side effects in terms of high toxicity and thus become ineffective. Sustained and controlled drug delivery systems, for delivering drugs at the infected site will be an optimal strategy. Recent studies revealed application of HAP nanoparticles for local drug delivery due to their superior biocompatibility, low toxicity, controllable physicochemical properties (composition,

particle size, porous structure, morphology), economical production, resistance to microbial degradation, storage stability, and pH responsive dissolution [194]. The drug absorption, release profile, and therapeutic effects of HAP nanoparticles are governed by characteristics of HAP viz. morphology, structure, pore size, and surface chemistry etc. [195].

Advancement in nanotechnology has opened new fields in biomedical applications with nanoparticles acting as drug delivery vehicles. This drug delivery system presents huge prospects in terms of drug localization at target site, regulated and sustained dosage, limiting drug toxicity to adjacent organs etc. Nanoparticles attributed to improved physicochemical properties, enhanced drug concentration to the target tissues with reduced side-effects, lower drug dosage requirement, high payload, sustained drug delivery [56]. Thus, HAP nanoparticles have emerged as viable solution to treat the infections by acting as nanocarriers for antibiotics [39], genes [40], proteins [41], and various drugs due to their superior biocompatibility, bioactivity, and nontoxicity [42, 43]. Reports suggested that nanodimensional HAP exhibited better interaction at implant–cell interface as compared with microndimensional particles [44]. Nanostructured hierarchical designs of HAP have shown high drug uptake and favorably release properties [55].

Some recent studies have reported that diverse nanostructures have different loading and releasing efficiencies for specific drugs [59]. Drug uptake, release characteristics, and thereafter therapeutic effects are governed by surface chemistry, porosity, surface area, and morphology of HAP nanoparticles. Therefore, amount of drug absorbed and its release profiles can be regulated by formulating desirable HAP nanostructures. Primarily, adsorption and desorption kinetics reliant on the precise properties of employed drug and structure of HAP nanoparticles [43]. In recent years, nanorods-like HAP morphology has been gaining lot of consideration due to its enhanced protein adsorption owing to greater charging surface efficiency [61]. Nanorods-like morphology of HAP exhibited favorable biocompatibility and bioactivity because of enhanced adsorbing ability, since the underlying Vander Waal interactions are enhanced due to large area offered by nanorods structure [11]. Researchers have reported that narrow particle morphology of nanorods was found to be more advantageous over spherical counterparts in targeted drug delivery applications, as these adhere more effectively to endothelial cells [60]. HAP nanorods functionalized with polyethylene glycol and folic acid showed directed drug delivery with initial burst release followed by prolonged release of anticancer drug, paclitaxel [196]. HAP with mesoporous structure possessed large surface area and large pore volume characteristics, having wide applications for targeted and controlled drug delivery systems [65]. Similarly, porous microspheres of HAP have reported 27–45% higher drug loading as compared with traditional HAP nanoparticles, whereas, drug release was sustained and prolonged [131].

Furthermore, doping of HAP nanoparticles with suitable ions have demonstrated enhanced drug loading and release characteristic together with enhancement of other desirable properties. Porous microspheres of Sr-doped HAP particles exhibited higher drug loading capability and persistent drug release properties for vancomycin drug due to their special characteristics involving novel hierarchical structure, mesoporous high surface area, and interactions of hydrogen bonding between drug and carrier [166]. Zhang et al. [62] synthesized multifunctional Sr-doped HAP particles with nanorods-like morphology with improved drug loading and controlled release properties for ibuprofen drug. Kim et al. demonstrated that Zn-doped HAP nanoparticles exhibited optimum drug loading efficiency and pH responsive drug release with MG-63 cell lines to treat the post operative bone cancer tissues [197]. Iron ($Fe^{3+)}$-doped HAP nanospheres with 75 nm diameter had shown effective anticancer and antibacterial activities, when loaded with amoxicillin and 5-fluorouracil and tested against *staphylococcus epidermidis*, *staphylococcus aureus*, *escherichia coli*, and cancerous cells (osteocarcoma cell line-MG63) [198]. Neodymium-doped HAP needle shaped nanoparticles loaded with doxorubicin hydrochloride demonstrated increased drug adsorption capability and sustained drug release profile along with excellent blood compatibility, cellular internalization properties, and inappreciable toxicity [199].

The characteristics of pH-dependent dissolution of drug delivery systems are particularly remarkable and can be potentially employed for targeted drug delivery applications. It has been noticed that degradation rate of HAP increases with decrease in pH from alkaline to acidic. The normal human body and healthy tissues have pH value of 7.4, whereas, extracellular environments like solid tumors may develop pH value round 5, thus pH-dependent and desirable drug release from HAP surface is helpful to treat tumors [194]. Previous investigations have demonstrated pH reactive release of doxorubicin in treating breast cancer cell lines BT20 [200]. HAP nanoparticles have been used as delivery agents for various drugs, such anticancer, antibiotics, anti-inflammatory, and proteins [131, 166, 200]. HAP incorporated with hydroxypropyl-β-cyclodextrin polymer (polyHP-βCD) showed sustained and controlled release of ciprofloxacin and vancomycin for the cure of bone related infections [201]. Table 4 lists different types of drugs and their behavior for pure and substituted materials with varied morphologies.

Thus, structural modification of HAP nanoparticles and their morphology may offer the wonderful opportunities

**Table 4** Drug delivery using HAP particles

| Material | Particle morphology | Drug name with its effect(s) | Drug behavior | References |
|---|---|---|---|---|
| Co-substituted (Na, Mg, K, F, Cl, and $CO_3^{2-}$) HAP | Porous microspheres | Ibuprofen, anti-inflammatory | Initial burst release followed by slow release | [131] |
| Strontium doped HAP | Microspheres | Vancomycin, antibiotic | Initial burst release followed by slow release | [166, 209] |
| Strontium substituted HAP | Mesoporous nanorods | Ibuprofen, anti-inflammatory | Initial burst release followed by slow release | [62] |
| Strontium substituted HAP | Fibrous crystallites | Amoxicillin | Controlled release | [210] |
| Silicon substituted HAP | Scaffolds | Vancomycin, antibiotic | First-order release kinetics | [211] |
| Zinc substituted HAP | Nanoparticles | Ciprofloxacin, anti-bacterial | Initial fast release followed by controlled release | [212] |
| Zinc and magnesium doped HAP | Nanoparticles | Bovine serum albumin (BSA) | Initial burst release followed by controlled release | [213] |
| Amorphous calcium phosphate | Porous nanospheres | Docetaxel, anticancer | Linear, slow and sustained release | [214] |
| Pure HAP | Hollow microspheres | Doxorubicin, anticancer | pH sensitive slow and sustained release | [215] |
| Pure HAP | Nanoparticles | Kiteplatin | pH sensitive release | [216] |
| Pure HAP | Microspheres | Chlorhexidine, antimicrobial | Sustained release | [217] |
| Pure HAP | Nanoparticles | Doxorubicin, anticancer | Linear release, quicker at low dosage | [218] |
| Pure HAP | Mesoporous nanoparticles | Doxorubicin, anticancer | First order pH sensitive release | [200] |
| Pure HAP | Hollow microspheres | Ibuprofen, anti-inflammatory | Initial rapid release followed by slow release | [177] |

and applications in the field of controlled drug delivery applications using HAP nanodevices.

#### 7.2.1 Drug release mechanism

It has been observed that the amount and drug release profile depends upon the rate of matrix degradation of HAP materials. Various attempts have been made to propose a valid mathematical model correlating the drug release with matrix degradation [202]. Three models are primarily used to determine the amount of drug release. These are named as first-order kinetics model, Gallagher–Corrigan model and Higuchi model. All these models depict the drug release kinetics under local environment and various reaction conditions.

1. The first-order kinetics model is used to describe the drug release from the porous matrices. General formula used for this model is given in Eq. (1):

$$f_t = f_{tmax}\left(1 - e^{-k_1 t}\right) \tag{1}$$

Where $f_t$ is the fraction of drug released in $t$ time, $f_{tmax}$ is the maximum fraction of drug released during the process and $k_1$ is the first-order kinetic constant ($h^{-1}$) [203].

2. The Gallagher–Corrigan model combines the two state model and most commonly used model to accurately describe the drug release. Briefly, it includes initial rapid release of the drug adherent to the matrix surface followed by a more controlled release from the matrix degradation. It is given by Eq. (2):

$$f_t = f_{tmax}\left(1 - e^{-k_1 t}\right) + \left(f_{tmax} - f_b\right).\frac{e^{-k_2 t - k_2 t_{2max}}}{1 + \left(e^{-k_2 t - k_2 t_{2max}}\right)}, \tag{2}$$

where $f_t$ is the fraction of drug release in $t$ time, $f_{tmax}$ is maximum fraction of drug released during process and $f_b$ is the fraction of drug released during 1st stage i.e., burst effect. $k_1$ is the first-order kinetic constant ($h^{-1}$) (1st stage of release), $k_2$ is the kinetic constant for 2nd stage of release process involving matrix degradation, and $t_{2max}$ is the time to maximum drug release rate (h) [204].

3. The Higuchi model is used for the analysis of drug release from swollen matrix. The general description is given by Eq. (3):

$$f_t = K_H \times t^{0.5}, \tag{3}$$

where $f_t$ is the fraction of drug released in $t$ time and $K_H$ is Higuchi dissolution constant [205].

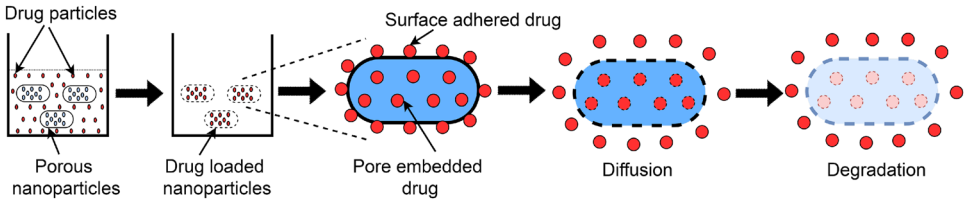


**Fig. 11** Drug release mechanism from HAP matrix

Any one or all models discussed, can be used to calculate drug release from HAP materials. However, Gallagher–Corrigan model is the most commonly used model to depict the drug release characteristics from HAP matrix. The general drug delivery mechanism from HAP matrix for nanorods is shown in Fig. 11. Initially, drug molecules adhered over the surface of HAP particles released in bulk amount, showing burst release effect. After some time, drug is released in a more controlled and sustained manner with the degradation of HAP matrix.

## 8 Conclusion

This review provides a detailed discussion on physicochemical, biological, and mechanical properties of HAP with the aim of tailoring these properties by altering the chemical composition, morphology, particle size, and suitable ionic substitutions. Though, some ionic substitutions have been extensively investigated by researchers, limited wok is available on the incorporation of alternative ions, not commonly found in natural apatite, which offers interesting challenges. To fully avail true benefits, a good understanding of desirable properties for these ionic substitutions is critically important. Among the various synthesis route available to fabricate the nanoparticles, hydrothermal and microwave-assisted synthesis techniques have been reported to be most promising with wide control on synthesis parameters to obtain final product with desirable properties. Furthermore, use of HAP particles with customized properties has been discussed for bone-tissue engineering and drug delivery applications. It has been found that bone regeneration and growth can be accelerated by controlling the physicochemical, morphological, and biological properties. In addition, it has been observed that morphology and porous structure of HAP particles have critical influence on the amount of loading and release characteristics for a particular drug. Synthesis of sustained and controlled drug delivery carriers for delivering drugs at the infected site(s) will be an optimal strategy. Overall, HAP is a classic material for biomedical applications with the necessity of further studies to revamp HAP and its properties for long-term in vivo applications.

**Author contributions** The manuscript was written through contributions of all authors. All authors have given approval to the final version of the paper.

## Compliance with ethical standards

**Conflict of interest** The authors declare that they have no conflict of interest.



## References

1. Suchanek W, Yoshimura M (1998) Processing and properties of hydroxyapatite-based biomaterials for use as hard tissue replacement implants. J Mater Res 13:94–117
2. Ratnayake JTB, Mucalo M, Dias GJ (2017) Substituted hydroxyapatites for bone regeneration: a review of current trends. J Biomed Mater Res—Part B Appl Biomater 105:1285–1299
3. Okazaki Y, Gotoh E (2005) Comparison of metal release from various metallic biomaterials in vitro. Biomaterials 26:11–21
4. Shastri V (2005) Non-degradable biocompatible polymers in medicine: past, present and future. Curr Pharm Biotechnol 4:331–337
5. Lyu S, Untereker D (2009) Degradability of polymers for implantable biomedical devices. Int J Mol Sci 10:4033–4065
6. Cui FZ, Li Y, Ge J (2007) Self-assembly of mineralized collagen composites. Mater Sci Eng R: Rep. 57:1–27
7. Murugan R, Ramakrishna S (2005) Development of nanocomposites for bone grafting. Compos Sci Technol 65:2385–2406
8. Kalita SJ, Bhardwaj A, Bhatt HA (2007) Nanocrystalline calcium phosphate ceramics in biomedical engineering. Mater Sci Eng C 27:441–449
9. Hench LL (1991) Bioceramics: from concept to clinic. J Am Ceram Soc 74:1487–1510
10. Arcos D, Vallet-Regi M (2013) Bioceramics for drug delivery. Acta Mater 61:890–911
11. Mayer C, Bagheri F, Zandi M, Urch H, Mirzadeh H, Eslaminejad MB, Mivehchi H (2009) Biocompatibility evaluation of nano-rod hydroxyapatite/gelatin coated with nano-HAp as a novel scaffold using mesenchymal stem cells. J Biomed Mater Res Part A 92A:1244–1255
12. Ghanaati S, Barbeck M, Detsch R, Deisinger U, Hilbig U, Rausch V, Sader R, Unger RE, Ziegler G, Kirkpatrick CJ (2012) The chemical composition of synthetic bone substitutes influences tissue reactions in vivo: Histological and histomorphometrical analysis of the cellular inflammatory response to hydroxyapatite, beta-tricalcium phosphate and biphasic calcium phosphate cer. Biomed Mater 7:1–14

13. Elliott JC (1994) Hydroxyapatite and nonstoichiometric apatites. In: Studies in inorganic chemistry. 111–189
14. Leventouri T (2006) Synthetic and biological hydroxyapatites: crystal structure questions. Biomaterials 27:3339–3342
15. Posner AS, Perloff A, Diorio AF (1958) Refinement of the hydroxyapatite structure. Acta Crystallogr 11:308–309
16. Boanini E, Gazzano M, Bigi A (2010) Ionic substitutions in calcium phosphates synthesized at low temperature. Acta Biomater 6:1882–1894
17. Wang L, Nancollas GH (2008) Calcium orthophosphates: crystallization and dissolution. Chem Rev 108:4628–4669
18. Vallet-Regí M, González-Calbet JM (2004) Calcium phosphates as substitution of bone-tissues. Prog Solid State Chem 32:1–31
19. Williams DF (2008) On the mechanisms of biocompatibility. Biomaterials 29:2941–2953
20. Yoshimura M, Suda H, Okamoto K, Ioku K (1994) Hydrothermal synthesis of biocompatible whiskers. J Mater Sci 29:3399–3402
21. Zhao Y, Zhang Y, Ning F, Guo D, Xu Z (2007) Synthesis and cellular biocompatibility of two kinds of HAP with different nanocrystal morphology. J Biomed Mater Res Part B, Appl Biomater 83:340–344
22. Vallet-Regí M (2001) Ceramics for medical applications. Dalton Trans 2:97–108
23. Albrektsson T, Johansson C (2001) Osteoinduction, osteoconduction and osseointegration. Eur Spine J 10:S96–S101
24. D' Elia NL, Mathieu C, Hoemann CD, Laiuppa JA, Santillan GE, Messina PV (2015) Bone-repair properties of biodegradable hydroxyapatite nano-rods superstructures. Nanoscale 7:18751–18762
25. Gautam CR, Kumar S, Biradar S, Jose S, Mishra VK (2016) Synthesis and enhanced mechanical properties of MgO substituted hydroxyapatite: a bone substitute material. RSC Adv 6:67565–67574
26. Bandyopadhyay A, Bernard S, Xue W, Böse S (2006) Calcium phosphate-based resorbable ceramics: Influence of MgO, ZnO, and $SiO_2$ dopants. J Am Ceram Soc 89:2675–2688
27. Curran DJ, Fleming TJ, Towler MR, Hampshire S (2011) Mechanical parameters of strontium doped hydroxyapatite sintered using microwave and conventional methods. J Mech Behav Biomed Mater 4:2063–2073
28. Bose S, Banerjee A, Dasgupta S, Bandyopadhyay A (2009) Synthesis, processing, mechanical, and biological property characterization of hydroxyapatite whisker-reinforced hydroxyapatite composites. J Am Ceram Soc 92:323–330
29. Li H, Song X, Li B, Kang J, Liang C, Wang H, Yu Z, Qiao Z (2017) Carbon nanotube-reinforced mesoporous hydroxyapatite composites with excellent mechanical and biological properties for bone replacement material application. Mater Sci Eng C 77:1078–1087
30. Dasgupta S, Tarafder S, Bandyopadhyay A, Bose S (2013) Effect of grain size on mechanical, surface and biological properties of microwave sintered hydroxyapatite. Mater Sci Eng C 33:2846–2854
31. Wang J, Shaw LL (2009) Nanocrystalline hydroxyapatite with simultaneous enhancements in hardness and toughness. Biomaterials 30:6565–6572
32. Ravi ND, Balu R, Sampath Kumar TS (2012) Strontium-substituted calcium deficient hydroxyapatite nanoparticles: Synthesis, characterization, and antibacterial properties. J Am Ceram Soc 95:2700–2708
33. Kim TN, Feng QL, Kim JO, Wu J, Wang H, Chen GC, Cui FZ (1998) Antimicrobial effects of metal ions (Ag+, $Cu^{2+}$, $Zn^{2+}$) in hydroxyapatite. J Mater Sci Mater Med 9:129–134
34. Kumar GS, Govindan R, Girija EK (2014) In situ synthesis, characterization and in vitro studies of ciprofloxacin loaded hydroxyapatite nanoparticles for the treatment of osteomyelitis. J Mater Chem B 2:5052–5060
35. Dorozhkin SV (2013) Calcium orthophosphate-based bioceramics. Materials 6:3840–3942
36. Lin K, Chang J (2015) Structure and properties of hydroxyapatite for biomedical applications. In: Hydroxyapatite (HAp) for biomedical applications, Elsevier Ltd. 3–19
37. Zhou H, Lee J (2011) Nanoscale hydroxyapatite particles for bone-tissue engineering. Acta Biomater 7:2769–2781
38. Ferraz MP, Monteiro FJ, Manuel CM (2004) Hydroxyapatite nanoparticles: a review of preparation methodologies. J Appl Biomater Biomech 2:74–80
39. Yang LX, Yin JJ, Wang LL, Xing GX, Yin P, Liu QW (2012) Hydrothermal synthesis of hierarchical hydroxyapatite: preparation, growth mechanism and drug release property. Ceram Int 38:495–502
40. Sereni A, Trombelli L, Mischiati C, del Senno L, Sibilla P, Banzi M, Manzati E, Aguiari G (2009) Effects of a hydroxyapatite-based biomaterial on gene expression in osteoblast-like cells. J Dent Res 85:354–358
41. Yuan X, Zhu B, Ma X, Tong G, Su Y, Zhu X (2013) Low temperature and template-free synthesis of hollow hydroxy zinc phosphate nanospheres and their application in drug delivery. Langmuir 29:12275–12283
42. Liu TY, Chen SY, Liu DM, Liou SC (2005) On the study of BSA-loaded calcium-deficient hydroxyapatite nano-carriers for controlled drug delivery. J Controlled Release 107:112–121
43. Palazzo B, Iafisco M, Laforgia M, Margiotta N, Natile G, Bianchi CL, Walsh D, Mann S, Roveri N (2007) Biomimetic hydroxyapatite-drug nanocrystals as potential bone substitutes with antitumor drug delivery properties. Adv Funct Mater 17:2180–2188
44. Park J, Lakes RS (2007) Biomaterials: an introduction. 3rd edn. Springer, USA
45. Webster TJ, Ergun C, Doremus RH, Siegel RW, Bizios R (2000) Enhanced functions of osteoblasts on nanophase ceramics. Biomaterials 21:1803–1810
46. Huang J, Best SM, Bonfield W, Brooks RA, Rushton N, Jayasinghe SN, Edirisinghe MJ (2004) In vitro assessment of the biological response to nano-sized hydroxyapatite. J Mater Sci: Mater Med 15:441–445
47. Shi Z, Huang X, Cai Y, Tang R, Yang D (2009) Size effect of hydroxyapatite nanoparticles on proliferation and apoptosis of osteoblast-like cells. Acta Biomater 5:338–345
48. Lemons JE, Catledge SA, Lacefield WR, Woodard S, Fries MD, Vohra YK, Venugopalanc R (2002) Nanostructured ceramics for biomedical implants. J Nanosci Nanotechnol 2:293–312
49. Webster TJ, Siegel RW, Bizios R (2001) Enhanced surface and mechanical properties of nanophase ceramics to achieve orthopaedic/dental implant efficacy. Key Eng Mater 192–195: 321–324
50. Okada M, Furukawa K, Serizawa T, Yanagisawa Y, Tanaka H, Kawai T, Furuzono T (2009) Interfacial interactions between calcined hydroxyapatite nanocrystals and substrates. Langmuir 25:6300–6306
51. Webster TJ, Ergun C, Doremus RH, Siegel RW, Bizios R (2000) Specific proteins mediate enhanced osteoblast adhesion on nanophase ceramics. J Biomed Mater Res 51:475–483
52. Hahn H (2003) Unique features and properties of nanostructured materials. Adv Eng Mater 5:277–284
53. Ramesh S, Tan CY, Bhaduri SB, Teng WD, Sopyan I (2008) Densification behaviour of nanocrystalline hydroxyapatite bioceramics. J Mater Process Technol 206:221–230
54. Padilla S, Izquierdo-Barba I, Vallet-Regí M (2008) High specific surface area in nanometric carbonated hydroxyapatite. Chem Mater 20:5942–5944

55. Zhao XY, Zhu YJ, Chen F, Lu BQ, Wu J (2013) Nanosheet-assembled hierarchical nanostructures of hydroxyapatite: surfactant-free microwave-hydrothermal rapid synthesis, protein/DNA adsorption and pH-controlled release. CrystEngComm 15:206–212
56. Yang L, Sheldon BW, Webster TJ (2010) Nanophase ceramics for improved drug delivery: current opportunities and challenges. Am Ceram Soc Bull 89:24–32
57. Padmanabhan SK, Balakrishnan A, Chu MC, Lee YJ, Kim TN, Cho SJ (2009) Sol-gel synthesis and characterization of hydroxyapatite nanorods. Particuology 7:466–470
58. Lin K, Chang J, Lu J, Wu W, Zeng Y (2007) Properties of β-$Ca_3(PO_4)_2$ bioceramics prepared using nano-size powders. Ceram Int 33:979–985
59. Guo YP, Yao YB, Ning CQ, Guo YJ, Chu LF (2011) Fabrication of mesoporous carbonated hydroxyapatite microspheres by hydrothermal method. Mater Lett 65:2205–2208
60. Agrawal S, Kelkar M, De A, Kulkarni AR, Gandhi MN (2016) Surfactant free novel one-minute microwave synthesis, characterization and cell toxicity study of mesoporous strontium hydroxyapatite nanorods. RSC Adv 6:94921–94926
61. Kawachi G, Sasaki S, Nakahara K, Ishida EH, Ioku K (2009) Porous apatite carrier prepared by hydrothermal method. Key Eng Mater 309–311:935–938
62. Zhang C, Li C, Huang S, Hou Z, Cheng Z, Yang P, Peng C, Lin J (2010) Self-activated luminescent and mesoporous strontium hydroxyapatite nanorods for drug delivery. Biomaterials 31:3374–3383
63. Grandjean-Laquerriere A, Laquerriere P, Laurent-Maquin D, Guenounou M, Phillips TM (2004) The effect of the physical characteristics of hydroxyapatite particles on human monocytes IL-18 production in vitro. Biomaterials 25:5921–5927
64. Kolhar P, Anselmo AC, Gupta V, Pant K, Prabhakarpandian B, Ruoslahti E, Mitragotri S (2013) Using shape effects to target antibody-coated nanoparticles to lung and brain endothelium. Proc Natl Acad Sci 110:10753–10758
65. Zhao P, Liu M-C, Lin H-C, Sun X-Y, Li Y-Y, Yan S-Q (2017) Synthesis and drug delivery applications for mesoporous silica nanoparticles. J Med Biotechnol 1:1–5
66. Shao F, Liu L, Fan K (2012) Ibuprofen loaded porous calcium phosphate nanospheres for skeletal drug delivery system. J Mater Sci 47:1054–1058
67. Murugan R, Ramakrishna S (2006) Designing biological apatite suitable for neomycin delivery. J Mater Sci 41:4343–4347
68. Le Huec JC, Schaeverbeke T, Clement D, Faber J, Le Rebeller A (1995) Influence of porosity on the mechanical resistance of hydroxyapatite ceramics under compressive stress. Biomaterials 16:113–118
69. Capuccini C, Torricelli P, Boanini E, Gazzano M, Giardino R, Bigi A (2009) Interaction of Sr-doped hydroxy apatite nanocrystals with osteoclast and osteoblast-like cells. J Biomed Mater Res—Part A 89:594–600
70. Bracci B, Torricelli P, Panzavolta S, Boanini E, Giardino R, Bigi A (2009) Effect of $Mg^{2+}$, $Sr^{2+}$, and $Mn^{2+}$ on the chemico-physical and in vitro biological properties of calcium phosphate biomimetic coatings. J Inorg Biochem 103:1666–1674
71. Legeros RZ (1993) Biodegradation and bioresorption phosphate ceramics of calcium. Clin Mater 14:65–88
72. Landi E, Tampieri A, Celotti G, Sprio S, Sandri M, Logroscino G (2007) Sr-substituted hydroxyapatites for osteoporotic bone replacement. Acta Biomater 3:961–969
73. Norhidayu D, Sopyan I, Ramesh S (2008) Development of zinc doped hydroxyapatite for bone implant applications. In: Proceedings of the International Conference on Construction and Building Technology 2008:257–270
74. Bianco A, Cacciotti I, Lombardi M, Montanaro L (2009) Si-substituted hydroxyapatite nanopowders: synthesis, thermal stability and sinterability. Mater Res Bull 44:345–354
75. Landi E, Tampieri A, Mattioli-Belmonte M, Celotti G, Sandri M, Gigante A, Fava P, Biagini G (2006) Biomimetic Mg- and $Mg_2CO_3$-substituted hydroxyapatites: synthesis characterization and in vitro behaviour. J Eur Ceram Soc 26:2593–2601
76. Kumta PN, Sfeir C, Lee DH, Olton D, Choi D (2005) Nanostructured calcium phosphates for biomedical applications: Novel synthesis and characterization. Acta Biomater 1:65–83
77. Yasukawa A, Ouchi S, Kandori K, Ishikawa T (1996) Preparation and characterization of magnesium-calcium hydroxyapatites. J Muter Chem 6:1401–1405
78. Bigi A, Falini G, Foresti E, Gazzano M, Ripamonti A, Roveri N (1996) Rietveld structure refinements of calcium hydroxylapatite containing magnesium. Acta Crystallogr Sect B: Struct Sci 52:87–92
79. Gibson IR, Bonfield W (2002) Preparation and characterization of magnesium/carbonate co-substituted hydroxyapatites. J Mater Sci: Mater Med 13:685–693
80. Landi E, Logroscino G, Proietti L, Tampieri A, Sandri M, Sprio S (2008) Biomimetic Mg-substituted hydroxyapatite: From synthesis to in vivo behaviour. J Mater Sci: Mater Med 19:239–247
81. Bertinetti L, Drouet C, Combes C, Rey C, Tampieri A, Coluccia S, Martra G (2009) Surface characteristics of nanocrystalline apatites: effect of Mg surface enrichment on morphology, surface hydration species, and cationic environments. Langmuir 25:5647–5654
82. Zyman Z, Tkachenko M, Epple M, Polyakov M, Naboka M (2006) Magnesium-substituted hydroxyapatite ceramics. Mater Werkst 37:474–477
83. Fadeev IV, Shvorneva LI, Barinov SM, Orlovskii VP (2003) Synthesis and structure of magnesium-substituted hydroxyapatite. Inorg Mater 39:947–950
84. Bigi A, Boanini E, Capuccini C, Gazzano M (2007) Strontium-substituted hydroxyapatite nanocrystals. Inorg Chim Acta 360:1009–1016
85. Verberckmoes SC, Behets GJ, Oste L, Bervoets AR, Lamberts LV, Drakopoulos M, Somogyi A, Cool P, Dorriné W, De Broe ME et al. (2004) Effects of strontium on the physicochemical characteristics of hydroxyapatite. Calcif Tissue Int 75:405–415
86. Shen Y, Liu J, Lin K, Zhang W (2012) Synthesis of strontium substituted hydroxyapatite whiskers used as bioactive and mechanical reinforcement material. Mater Lett 70:76–79
87. Kim HW, Koh YH, Kong YM, Kang JG, Kim HE (2004) Strontium substituted calcium phosphate biphasic ceramics obtained by a powder precipitation method. J Mater Sci: Mater Med 15:1129–1134
88. Kavitha M, Subramanian R, Narayanan R, Udhayabanu V (2014) Solution combustion synthesis and characterization of strontium substituted hydroxyapatite nanocrystals. Powder Technol 253:129–137
89. Ovesen J, Moller-Madsen B, Thomsen JS, Danscher G, Mosekilde L (2001) The positive effects of zinc on skeletal strength in growing rats. Bone 29:565–570
90. Hall SL, Dimai HP, Farley JR (1999) Effects of zinc on human skeletal alkaline phosphatase activity in vitro. Calcif Tissue Int 64:163–172
91. Yamaguchi M (1998) Role of Zinc in Bone Formation and Bone Resorption. J Trace Elem Exp Med 11:119–135
92. Miao S, Cheng K, Weng W, Du P, Shen G, Han G, Yan W, Zhang S (2008) Fabrication and evaluation of Zn containing fluoridated hydroxyapatite layer with Zn release ability. Acta Biomater 4:441–446

93. Ren F, Xin R, Ge X, Leng Y (2009) Characterization and structural analysis of zinc-substituted hydroxyapatites. Acta Biomater 5:3141–3149
94. Bigi A, Foresti E, Gandolfi M, Gazzano M, Roveri N (1997) Isomorphous substitutions in β-tricalcium phosphate: The different effects of zinc and strontium. J Inorg Biochem 66:259–265
95. Kaygili O, Tatar C (2012) The investigation of some physical properties and microstructure of Zn-doped hydroxyapatite bioceramics prepared by sol-gel method. J Sol–Gel Sci Technol 61:296–309
96. Jallot E, Nedelec JM, Grimault AS, Chassot E, Grandjean-Laquerriere A, Laquerriere P, Laurent-Maquin D (2005) STEM and EDXS characterisation of physico-chemical reactions at the periphery of sol-gel derived Zn-substituted hydroxyapatites during interactions with biological fluids. Colloids Surf B: Biointerfaces 42:205–210
97. Yingguang L, Zhuoru Y, Jiang C (2007) Preparation, characterization and antibacterial property of cerium substituted hydroxyapatite nanoparticles. J Rare Earths 25:452–456
98. Feng Z, Liao Y, Ye M (2005) Synthesis and structure of cerium-substituted hydroxyapatite. J Mater Sci: Mater Med 16:417–421
99. Reardon PJT, Huang J, Tang J (2013) Morphology controlled porous calcium phosphate nanoplates and nanorods with enhanced protein loading and release functionality. Adv Healthc Mater 2:682–686
100. Medvecký Ľ, Štulajterová R, Parilák Ľ, Trpčevská J, Ďurišin J, Barinov SM (2006) Influence of manganese on stability and particle growth of hydroxyapatite in simulated body fluid. Colloids Surf A: Physicochem Eng Asp 281:221–229
101. Suitch PR (1985) The structural location and role of $Mn^{2+}$ partially substituted for $Ca^{2+}$ in fluorapatite. Acta Cryst 41:173–179
102. Mayer I, Jacobsohn O, Niazov T, Werckmann J, Iliescu M, Richard-Plouet M, Burghaus O, Reinen D (2003) Manganese in precipitated hydroxyapatites. Eur J Inorg Chem 2003:1445–1451
103. Mayer I, Schleich Y, Gdalya S, Reinen D, Burghaus O, Popov I, Cuisinier FJG (2006) Phase relations between β-tricalcium phosphate and hydroxyapatite with manganese(II): structural and spectroscopic properties. Eur J Inorg Chem 7:1460–1465
104. Li Y, TeckNam C, PingOoi C (2009) Iron(III) and manganese(II) substituted hydroxyapatite nanoparticles: characterization and cytotoxicity analysis. J Phys: Conf Ser 187:012024
105. Bigi A, Bracci B, Cuisinier F, Elkaim R, Fini M, Mayer I, Mihailescu IN, Socol G, Sturba L, Torricelli P (2005) Human osteoblast response to pulsed laser deposited calcium phosphate coatings. Biomaterials 26:2381–2389
106. LeGeros R (1965) Effect of carbonate on lattice parameters of apatite. Nature 835–837
107. Lacout J, Nounah A, Ferhat M (1998) Strontium-cadmium substitution in hydroxyl and fluorapatites. Ann Chem Sci Mater 23:57–60
108. Shimoda S, Aoba T, Moreno EC, Miake Y (1990) Effect of solution composition on morphological and structural features of carbonated calcium apatites. J Dent Res 69:1731–1740
109. Murugan R, Ramakrishna S (2006) Production of ultra-fine bioresorbable carbonated hydroxyapatite. Acta Biomater 2:201–206
110. Ślósarczyk A, Paszkiewicz Z, Paluszkiewicz C (2005) FTIR and XRD evaluation of carbonated hydroxyapatite powders synthesized by wet methods. J Mol Struct 744–747:657–661
111. Qu H, Wei M (2006) The effect of fluoride contents in fluoridated hydroxyapatite on osteoblast behavior. Acta Biomater 2:113–119
112. Ten Cate JM, Featherstone JDB (1991) Mechanistic aspects of the interactions between fluoride and dental enamel. Crit Rev Oral Biol Med 2:283–296
113. Legeros RZ, Silverstone LM, Daculsi G, Kerebel LM (1983) In vitro caries-like lesion formation in F-containing tooth enamel. J Dent Res 62:138–144
114. Qu H, Wei M (2005) Synthesis and characterization of fluorine-containing hydroxyapatite by a pH-cycling method. J Mater Sci: Mater Med 16:129–133
115. Chen Y, Miao X (2005) Thermal and chemical stability of fluorohydroxyapatite ceramics with different fluorine contents. Biomaterials 26:1205–1210
116. Vallet-Regi M, Arcos D (2005) Silicon substituted hydroxyapatites. A method to upgrade calcium phosphate based implants. J Mater Chem 15:1509–1516
117. Tang XL, Xiao XF, Liu RF (2005) Structural characterization of silicon-substituted hydroxyapatite synthesized by a hydrothermal method. Mater Lett 59:3841–3846
118. Aminian A, Solati-Hashjin M, Samadikuchaksaraei A, Bakhshi F, Gorjipour F, Farzadi A, Moztarzadeh F, Schmücker M (2011) Synthesis of silicon-substituted hydroxyapatite by a hydrothermal method with two different phosphorous sources. Ceram Int 37:1219–1229
119. Porter AE, Patel N, Skepper JN, Best SM, Bonfield W (2003) Comparison of in vivo dissolution processes in hydroxyapatite and silicon-substituted hydroxyapatite bioceramics. Biomaterials 24:4609–4620
120. Sprio S, Tampieri A, Landi E, Sandri M, Martorana S, Celotti G, Logroscino G (2008) Physico-chemical properties and solubility behaviour of multi-substituted hydroxyapatite powders containing silicon. Mater Sci Eng C 28:179–187
121. Porter AE, Best SM, William B (2003) Ultrastructural comparison of hydroxyapatite and silicon-substituted hydroxyapatite for biomedical applications. J Biomed Mater Res 68A:133–141
122. Botelho CM, Brooks RA, Best SM, Lopes MA, Santos JD, Rushton N,WB (2006) Human osteoblast response to silicon-substituted hydroxyapatite. J Biomed Mater Res A 79:723–730
123. Pietak AM, Reid JW, Stott MJ, Sayer M (2007) Silicon substitution in the calcium phosphate bioceramics. Biomaterials 28:4023–4032
124. Bang LT, Ishikawa K, Othman R (2011) Effect of silicon and heat-treatment temperature on the morphology and mechanical properties of silicon-substituted hydroxyapatite. Ceram Int 37:3637–3642
125. Kim SR, Lee JH, Kim YT, Riu DH, Jung SJ, Lee YJ, Chung SC, Kim YH (2003) Synthesis of Si, Mg substituted hydroxyapatites and their sintering behaviors. Biomaterials 24:1389–1398
126. Gasquères G, Bonhomme C, Maquet J, Babonneau F, Hayakawa S, Kanaya T, Osaka A (2008) Revisiting silicate substituted hydroxyapatite by solid-state NMR. Magn Reson Chem 46:342–346
127. Lilja M, Lindahl C, Xia W, Engqvist H, Strømme M (2013) The effect of Si-doping on the release of antibiotic from hydroxyapatite coatings. J Biomater Nanobiotechnol 04:237–241
128. Markovich D (2001) Physiological roles and regulation of mammalian sulfate transporters. Physiol Rev 81:1499–1533
129. Alshemary AZ, Goh YF, Akram M, Razali IR, Abdul Kadir MR, Hussain R (2013) Microwave assisted synthesis of nano sized sulphate doped hydroxyapatite. Mater Res Bull 48:2106–2110
130. Toyama T, Kameda S (2013) Synthesis of sulfate-ion-substituted hydroxyapatite from amorphous calcium phosphate. Bioceram Dev Appl 3:10–12
131. Lin K, Qu H, Zhou Y, Chen F, Zhu Y, Chang J, Zhou Y (2011) Biomimetic hydroxyapatite porous microspheres with co-substituted essential trace elements: surfactant-free hydrothermal synthesis, enhanced degradation and drug release. J Mater Chem 21:16558–16565
132. Imrie FE, Aina V, Lusvardi G, Malavasi G, Gibson IR, Cerrato G, Annaz B (2013) Synthesis and characterisation of strontium

and magnesium co-substituted biphasic calcium phosphates. Key Eng Mater 529–530:88–93
133. Nsar S, Hassine A, Bouzouita K (2013) Sintering and mechanical properties of magnesium and fluorine co-substituted hydroxyapatites. J Biomater Nanobiotechnol 04:1–11
134. Gopi D, Ramya S, Rajeswari D, Karthikeyan P, Kavitha L (2014) Strontium, cerium co-substituted hydroxyapatite nanoparticles: Synthesis, characterization, antibacterial activity towards prokaryotic strains and in vitro studies. Colloids Surf A: Physicochem Eng Asp 451:172–180
135. Zhang N, Zhai D, Chen L, Zou Z, Lin K, Chang J (2014) Hydrothermal synthesis and characterization of Si and Sr co-substituted hydroxyapatite nanowires using strontium containing calcium silicate as precursors. Mater Sci Eng C 37:286–291
136. Manafi S, Joughehdoust S, Badiee SH (2009) Effect of pH on morphology, size and composition of calcium phosphate phase obtained in wet chemical. Int J Nanomanuf 5:169–178
137. Bezzi G, Celotti G, Landi E, La Torretta TMG, Sopyan I, Tampieri A (2003) A novel sol-gel technique for hydroxyapatite preparation. Mater Chem Phys 78:816–824
138. Zhu R, Yu R, Yao J, Wang D, Ke J (2008) Morphology control of hydroxyapatite through hydrothermal process. J Alloy Compd 457:555–559
139. Nasiri-Tabrizi B, Honarmandi P, Ebrahimi-Kahrizsangi R, Honarmandi P (2009) Synthesis of nanosize single-crystal hydroxyapatite via mechanochemical method. Mater Lett 63:543–546
140. Mishra VK, Srivastava SK, Asthana BP, Kumar D (2012) Structural and spectroscopic studies of hydroxyapatite nanorods Formed via microwave-assisted synthesis route. J Am Ceram Soc 95:2709–2715
141. Sl PM, Ashok M, Balasubramanian T, Riyasdeen A, Akbarsha MA (2009) Synthesis and characterization of nano-hydroxyapatite at ambient temperature using cationic surfactant. Mater Lett 63:2123–2125
142. Hong Y, Fan H, Li B, Guo B, Liu M, Zhang X (2010) Fabrication, biological effects, and medical applications of calcium phosphate nanoceramics. Mater Sci Eng R: Rep. 70:225–242
143. Bigi A, Boanini E, Rubini K (2004) Hydroxyapatite gels and nanocrystals prepared through a sol-gel process. J Solid State Chem 177:3092–3098
144. Li B, Chen X, Guo B, Wang X, Fan H, Zhang X (2009) Fabrication and cellular biocompatibility of porous carbonated biphasic calcium phosphate ceramics with a nanostructure. Acta Biomater 5:134–143
145. Sun Y, Guo G, Tao D, Wang Z (2007) Reverse microemulsion-directed synthesis of hydroxyapatite nanoparticles under hydrothermal conditions. J Phys Chem Solids 68:373–377
146. Coreño AJ, Coreño AO, Cruz RJJ, Rodríguez CC (2005) Mechanochemical synthesis of nanocrystalline carbonate-substituted hydroxyapatite. Optical Mater 27:1281–1285
147. Cao LY, Zhang CB, Huang JF (2005) Synthesis of hydroxyapatite nanoparticles in ultrasonic precipitation. Ceram Int 31:1041–1044
148. Qi Y, Shen J, Jiang Q, Bo J, Chen J, Zhang X (2015) The morphology control of hydroxyapatite microsphere at high pH values by hydrothermal method. Adv Powder Technol 26:1041–1046
149. Hassan MN, Mahmoud MM, El-Fattah AA, Kandil S (2016) Microwave-assisted preparation of Nano-hydroxyapatite for bone substitutes. Ceram Int 42:3725–3744
150. Farzadi A, Solati-Hashjin M, Bakhshi F, Aminian A (2011) Synthesis and characterization of hydroxyapatite/β-tricalcium phosphate nanocomposites using microwave irradiation. Ceram Int 37:65–71
151. Byrappa K, Adschiri T (2007) Hydrothermal technology for nanotechnology. Prog Cryst Growth Charact Mater 53:117–166
152. Liu J, Ye X, Wang H, Zhu M, Wang B, Yan H (2003) The influence of pH and temperature on the morphology of hydroxyapatite synthesized by hydrothermal method. Ceram Int 29:629–633
153. Sadat-shojai M, Khorasani M, Dinpanah-khoshdargi E, Jamshidi A (2013) Synthesis methods for nanosized hydroxyapatite with diverse structures. Acta Biomater 9:7591–7621
154. Yoshimura MBK (2008) Hydrothermal processing of materials: past, present and future. J Mater Sci 43:2085–2103
155. Chandanshive BB, Rai P, Rossi ALR, Ersen O, Khushalani D (2013) Synthesis of hydroxyapatite for biomedical applications. Mater Sci Eng C 33:2981–2986
156. Chen F, Zhu YJ, Wang KW, Zhao KLe (2011) Surfactant-free solvothermal synthesis of hydroxyapatite nanowire/nanotube ordered arrays with biomimetic structures. CrystEngComm 13:1858–1863
157. Lee DK, Park JY, Kim MR, Jang DJ (2011) Facile hydrothermal fabrication of hollow hexagonal hydroxyapatite prisms. CrystEngComm 13:5455–5459
158. Lester E, Tang SVY, Khlobystov A, Rose VL, Buttery L, Roberts CJ (2013) Producing nanotubes of biocompatible hydroxyapatite by continuous hydrothermal synthesis. CrystEngComm 15:3256–3260
159. Ma MG, Zhu YJ, Chang J (2008) Solvothermal preparation of hydroxyapatite microtubes in water/N,N-dimethylformamide mixed solvents. Mater Lett 62:1642–1645
160. Yan L, Li Y, Deng Z, Zhuang J, Sun X (2001) Surfactant-assisted hydrothermal synthesis of hydroxyapatite nanorods. Int J Inorg Mater 3:633–637
161. Sadat-Shojai M, Atai M, Nodehi A (2011) Design of experiments (DOE) for the optimization of hydrothermal synthesis of hydroxyapatite nanoparticles. J Braz Chem Soc 22:571–582
162. Zhu Y, Xu L, Liu C, Zhang C, Wu N (2018) Nucleation and growth of hydroxyapatite nanocrystals by hydrothermal method. AIP Adv 8:1–11
163. Bricha M, Belmamouni Y, Essassi EM, Ferreira JMF, Mabrouk K, El (2012) Surfactant-assisted hydrothermal synthesis of hydroxyapatite nanopowders. J Nanosci Nanotechnol 12:8042–8049
164. Giang LT, Hoai TT, Binh BTT, Nga NK, Tuan PNM, Huy TQ (2017) Hydrothermal synthesis of hydroxyapatite nanorods for rapid formation of bone-like mineralization. J Electron Mater 46:5064–5072
165. Pan HB, Li ZY, Lam WM, Wong JC, Darvell BW, Luk KDK, Lu WW (2009) Solubility of strontium-substituted apatite by solid titration. Acta Biomater 5:1678–1685
166. Lin K, Liu P, Wei L, Zou Z, Zhang W, Qian Y, Shen Y, Chang J (2013) Strontium substituted hydroxyapatite porous microspheres: surfactant-free hydrothermal synthesis, enhanced biological response and sustained drug release. Chem Eng J 222:49–59
167. Earl JS, Wood DJ, Milne SJ (2006) Hydrothermal synthesis of hydroxyapatite. J Phys 26:268–271
168. Lak A, Mazloumi M, Mohajerani MS, Zanganeh S, Shayegh MR, Kajbafvala A, Arami H, Sadrnezhaad SK (2008) Rapid formation of mono-dispersed hydroxyapatite nanorods with narrow-size distribution via microwave irradiation. J Am Ceram Soc 91:3580–3584
169. Mishra VK, Rai SB, Asthana BP, Parkash O, Kumar D (2014) Effect of annealing on nanoparticles of hydroxyapatite synthesized via microwave irradiation: structural and spectroscopic studies. Ceram Int 40:11319–11328
170. Kumar AR, Kalainathan S, Saral AM (2010) Microwave assisted synthesis of hydroxyapatite nano strips. Cryst Res Technol 45:776–778

171. Liu J, Li K, Wang H, Zhu M, Yan H (2004) Rapid formation of hydroxyapatite nanostructures by microwave irradiation. Chem Phys Lett 396:429–432
172. Iqbal N, Rafiq M, Kadir A, Ahmad N, Nik N, Humaimi N, Raman M, Kamarul T (2012) Rapid microwave assisted synthesis and characterization of nanosized silver-doped hydroxyapatite with antibacterial properties. Mater Lett 89:118–122
173. Wang YZ, Fu Y (2011) Microwave-hydrothermal synthesis and characterization of hydroxyapatite nanocrystallites. Mater Lett 65:3388–3390
174. Siddharthan A, Seshadri SK, Kumar TSS (2006) Influence of microwave power on nanosized hydroxyapatite particles. Scr Mater 55:175–178
175. Silva CC, Graça MPF, Valente MA, Góes JC, Sombra ASB (2006) Microwave preparation, structure and electrical properties of calcium–sodium–phosphate biosystem. J Non-Cryst Solids 352:3512–3517
176. Vani R, Raja SB, Sridevi TS, Savithri K, Devaraj SN, Girija EK, Thamizhavel A, Kalkura SN (2011) Surfactant free rapid synthesis of hydroxyapatite nanorods by a microwave irradiation method for the treatment of bone infection. Nanotechnology 22:285701
177. Qi C, Zhu YJ, Lu BQ, Zhao XY, Zhao J, Chen F, Wu J (2013) Hydroxyapatite hierarchically nanostructured porous hollow microspheres: Rapid, sustainable microwave-hydrothermal synthesis by using creatine phosphate as an organic phosphorus source and application in drug delivery and protein adsorption. Chem Eur J 19:5332–5341
178. Zhao XY, Zhu YJ, Qi C, Chen F, Lu BQ, Zhao J, Wu J (2013) Hierarchical hollow hydroxyapatite microspheres: Microwave-assisted rapid synthesis by using pyridoxal-5′-phosphate as a phosphorus source and application in drug delivery. Chem Asian J 8:1313–1320
179. Pal R, Maninder S, Mehta S, Shukla S, Singh S (2017) Influence of microwave power and irradiation time on some properties of hydroxyapatite nanopowders. J Sol–Gel Sci Technol 84:332–340
180. Yang Z, Jiang Y, Wang YJ, Ma LY, Li F (2004) Preparation and thermal stability analysis of hydroxyapatite derived from the precipitation process and microwave irradiation method. Mater Lett 58:3586–3590
181. Akram M, Alshemary AZ, Goh YF, Wan Ibrahim WA, Lintang HO, Hussain R (2015) Continuous microwave flow synthesis of mesoporous hydroxyapatite. Mater Sci Eng C 56:356–362
182. Wang KW, Zhu YJ, Chen F, Cheng GF, Huang YH (2011) Microwave-assisted synthesis of hydroxyapatite hollow microspheres in aqueous solution. Mater Lett 65:2361–2363
183. Fang Y, Agrawal DK, Roy DM, Roy R (1994) Microwave sintering of hydroxyapatite ceramics. J Mater Res 9:180–187
184. Cao JM, Feng J, Deng SG, Chang X, Wang J, Liu JS, Lu P, Lu HX, Zheng MB, Zhang F et al. (2005) Microwave-assisted solid-state synthesis of hydroxyapatite nanorods at room temperature. J Mater Sci 40:6311–6313
185. Wang H, Liu J, Li K, Wang H, Zhu M, Xu H (2005) Self-assembly of hydroxyapatite nanostructures by microwave irradiation. Nanotechnology 16:82–87
186. Nathanael AJ, Hong SI, Mangalaraj D, Ponpandian N, Chen PC (2012) Template-free growth of novel hydroxyapatite nanorings: Formation mechanism and their enhanced functional properties. Cryst Growth Des 12:3565–3574
187. Wang A, Yin H, Liu D, Wu H, Wada Y, Ren M, Xu Y, Jiang T, Cheng X (2007) Effects of organic modifiers on the size-controlled synthesis of hydroxyapatite nanorods. Appl Surf Sci 253:3311–3316
188. Arami H, Mohajerani M, Mazloumi M, Khalifehzadeh R, Lak A, Sadrnezhaad SK (2009) Rapid formation of hydroxyapatite nanostrips via microwave irradiation. J Alloy Compd 469:391–394
189. Wu X, Song X, Li D, Liu J, Zhang P, Chen X (2012) Preparation of mesoporous nano-hydroxyapatite using a surfactant template method for protein delivery. J Bionic Eng 9:224–233
190. Shin Y, Aoki H, Yoshiyama N, Akao M, Higashikata M (1992) Surface properties of hydroxyapatite ceramic as new percutaneous material in skin tissue. J Mater Sci: Mater Med 3:219–221
191. Wu P, Grainger DW (2006) Drug/device combinations for local drug therapies and infection prophylaxis. Biomaterials 27:2450–2467
192. Matsunaga K, Murata H, Mizoguchi T, Atsushi Nakahira (2010) Mechanism of incorporation of zinc into hydroxyapatite. Acta Biomater 6:2289–2293
193. Popat KC, Eltgroth M, LaTempa TJ, Grimes CA, Desai TA (2007) Decreased *Staphylococcus epidermis* adhesion and increased osteoblast functionality on antibiotic-loaded titania nanotubes. Biomaterials 28:4880–4888
194. Rodríguez-Ruiz I, Delgado-López JM, Durán-Olivencia MA, Iafisco M, Tampieri A, Colangelo D, Prat M, Gómez-Morales J (2013) PH-responsive delivery of doxorubicin from citrate-apatite nanocrystals with tailored carbonate content. Langmuir 29:8213–8221
195. Lin K, Chen L, Liu P, Zou Z, Zhang M, Shen Y, Qiao Y, Liu X, Chang J (2013) Hollow magnetic hydroxyapatite microspheres with hierarchically mesoporous microstructure for pH-responsive drug delivery. CrystEngComm 15:2999–3008
196. Venkatasubbu GD, Ramasamy S, Avadhani GS, Ramakrishnan V, Kumar J (2013) Surface modification and paclitaxel drug delivery of folic acid modified polyethylene glycol functionalized hydroxyapatite nanoparticles. Powder Technol 235:437–442
197. Kim H, Mondal S, Bharathiraja S, Manivasagan P, Moorthy MS, Oh J (2018) Optimized Zn-doped hydroxyapatite/doxorubicin bioceramics system for efficient drug delivery and tissue engineering application. Ceram Int 44:6062–6071
198. Chandra VS, Baskar G, Suganthi RV, Elayaraja K, Joshy MIA, Beaula WS, Mythili R, Venkatraman G, Kalkura SN (2012) Blood compatibility of iron-doped nanosize yydroxyapatite and its drug release. ACS Appl Mater Interfaces 4:1200–1210
199. Victor SP, Paul W, Jayabalan M, Sharma CP (2014) Supramolecular hydroxyapatite complexes as theranostic near-infrared luminescent drug carriers. CrystEngComm 16:9033–9042
200. Yang YH, Liu CH, Liang YH, Lin FH, Wu KCW (2013) Hollow mesoporous hydroxyapatite nanoparticles (hmHANPs) with enhanced drug loading and pH-responsive release properties for intracellular drug delivery. J Mater Chem B 1:2447–2450
201. Leprêtre S, Chai F, Hornez JC, Vermet G, Neut C, Descamps M, Hildebrand HF, Martel B (2009) Prolonged local antibiotics delivery from hydroxyapatite functionalised with cyclodextrin polymers. Biomaterials 30:6086–6093
202. Dion A, Langman M, Hall G, Filiaggi M (2005) Vancomycin release behaviour from amorphous calcium polyphosphate matrices intended for osteomyelitis treatment. Biomaterials 26:7276–7285
203. Dash S, Murthy PN, Nath L, Chowdhury P (2010) Kinetic modeling on drug release from controlled drug delivery systems. Acta Poloniae Pharm-Drug Res 67:217–223
204. Balcerzak J, Mucha M (2010) Analysis of model drug release kinetics from complex matrices of polylactide-chitosane. Prog Chem Appl Chitin Derivatives 15:117–126
205. Jarosz M, Pawlik A, Szuwarzyński M, Jaskuła M, Sulka GD (2016) Nanoporous anodic titanium dioxide layers as potential drug delivery systems: Drug release kinetics and mechanism. Colloids Surf B: Biointerfaces 143:447–454

206. Heimann RB (2013) Structure, properties, and biomedical performance of osteoconductive bioceramic coatings. Surf Coat Technol 233:27–38
207. Rouquerol J, Avnir D, Fairbridge CW, Everett DH, Haynes JH, Pernicone N, Ramsay JDF, Sing KSW, Unger KK (1994) Recommendations for the characterization of porous solids (Technical Report). Pure Appl Chem 66:1739–1758
208. Basirun WJ, Nasiri-Tabrizi B, Baradaran S (2018) Overview of hydroxyapatite–graphene nanoplatelets composite as bone graft substitute: mechanical behavior and in-vitro biofunctionality. Crit Rev Solid State Mater Sci 43:177–212
209. Jiang F, Wang DP, Ye S, Zhao X (2014) Strontium-substituted, luminescent and mesoporous hydroxyapatite microspheres for sustained drug release. J Mater Sci: Mater Med 25:391–400
210. Suganthi RV, Elayaraja K, Joshy MIA, Chandra VS, Girija EK, Kalkura SN (2011) Fibrous growth of strontium substituted hydroxyapatite and its drug release. Mater Sci Eng C 31:593–599
211. Martínez-vázquez FJ, Cabañas MV, Paris JL, Lozano D, Vallet-regí M (2015) Fabrication of novel Si-doped hydroxyapatite/gelatine scaffolds by rapid prototyping for drug delivery and bone regeneration. Acta Biomater 15:200–209
212. Devanand Venkatasubbu G, Ramasamy S, Ramakrishnan V, Kumar J (2011) Nanocrystalline hydroxyapatite and zinc-doped hydroxyapatite as carrier material for controlled delivery of ciprofloxacin. 3 Biotech 1:173–186
213. Dasgupta S, Banerjee SS, Bandyopadhyay A, Bose S (2010) Zn- and Mg-doped hydroxyapatite nanoparticles for controlled release of protein. Langmuir 26:4958–4964
214. Qi C, Zhu YJ, Zhao XY, Lu BQ, Tang QL, Zhao J, Chen F (2013) Highly stable amorphous calcium phosphate porous nanospheres: Microwave-assisted rapid synthesis using ATP as phosphorus source and stabilizer, and their application in anticancer drug delivery. Chem Eur J 19:981–987
215. Lai W, Chen C, Ren X, Lee IS, Jiang G, Kong X (2016) Hydrothermal fabrication of porous hollow hydroxyapatite microspheres for a drug delivery system. Mater Sci Eng C 62:166–172
216. Lelli M, Roveri N, Marzano C, Hoeschele JD, Curci A, Margiotta N, Gandin V, Natile G (2016) Hydroxyapatite nanocrystals as a smart, pH sensitive, delivery system for kiteplatin. Dalton Trans 45:13187–13195
217. Soriano-Souza CA, Rossi AL, Mavropoulos E, Hausen MA, Tanaka MN, Calasans-Maia MD, Granjeiro JM, Rocha-Leão MHM, Rossi AM (2015) Chlorhexidine-loaded hydroxyapatite microspheres as an antimicrobial delivery system and its effect on in vivo osteo-conductive properties. J Mater Sci: Mater Med 26:166–180
218. Kundu B, Ghosh D, Sinha MK, Sen PS, Balla VK, Das N, Basu D (2013) Doxorubicin-intercalated nano-hydroxyapatite drug-delivery system for liver cancer: an animal model. Ceram Int 39:9557–9566